AFRL-AFOSR-JP-TR-2024-0039

Elevon Control Power Effective of VTOL Tail-sitter in Hover Mode

CHINNAPAT THIPYOPAS
KASETSART UNIVERSITY
50 NGAM WONG WAN ROAD
CHATUCHAK, , 10900
THA

01/08/2024
Final Technical Report

Air Force Research Laboratory
Air Force Office of Scientific Research
Asian Office of Aerospace Research and Development
Unit 45002, APO AP 96338-5002

REPORT DOCUMENTATION PAGE

PLEASE DO NOT RETURN YOUR FORM TO THE ABOVE ORGANIZATION.

1. REPORT DATE	2. REPORT TYPE	3. DATES COVERED	
20240108	Final	START DATE 20210930	END DATE 20230929

4. TITLE AND SUBTITLE
Elevon Control Power Effective of VTOL Tail-sitter in Hover Mode

5a. CONTRACT NUMBER	5b. GRANT NUMBER	5c. PROGRAM ELEMENT NUMBER
	FA2386-21-1-4044	
5d. PROJECT NUMBER	**5e. TASK NUMBER**	**5f. WORK UNIT NUMBER**

6. AUTHOR(S)
Chinnapat Thipyopas

7. PERFORMING ORGANIZATION NAME(S) AND ADDRESS(ES)
KASETSART UNIVERSITY
50 NGAM WONG WAN ROAD
CHATUCHAK 10900
THA

8. PERFORMING ORGANIZATION REPORT NUMBER

9. SPONSORING/MONITORING AGENCY NAME(S) AND ADDRESS(ES)	10. SPONSOR/MONITOR'S ACRONYM(S)	11. SPONSOR/MONITOR'S REPORT NUMBER(S)
AOARD UNIT 45002 APO AP 96338-5002	AFRL/AFOSR IOA	AFRL-AFOSR-JP-TR-2024-0039

12. DISTRIBUTION/AVAILABILITY STATEMENT
A Distribution Unlimited: PB Public Release

13. SUPPLEMENTARY NOTES

14. ABSTRACT
The project aimes to assess the control power and efficiency of the control surface at the trailing edge of tail-sitter VTOL called Elevon. It leverages the advantage of mitigating propwash induced flow from the propeller blowing pass into the control surface on the wing's trailing edge to control its attitude. Hoever, stability issues arise during the vertical hovering and in particular in landing phase. The investigation focuses on determining the optimal installation position of propeller, size of propeller, and size of control surface through laboratory experiments. The results showed the sizing of propeller 15inch and 33.3%C control surface gives the highest pitching moment. Testing with the wind coming from the trailing edge, the pitching moment can be reduced up to 50% during landing phase. While current achivements are confined to the laboratory experiments, those contribute to enhancing UAV and AAM platform efficiency.

15. SUBJECT TERMS

16. SECURITY CLASSIFICATION OF:			17. LIMITATION OF ABSTRACT	18. NUMBER OF PAGES
a. REPORT U	b. ABSTRACT U	c. THIS PAGE U	SAR	1

19a. NAME OF RESPONSIBLE PERSON	19b. PHONE NUMBER *(Include area code)*
FUMIO KOJIMA	315-227-7007

Standard Form 298 (Rev.5/2020)
Prescribed by ANSI Std. Z39.18

Final Report

FA2386-21-1-4044

A.5.b. Asian Office of Aerospace Research and Development

Elevon Control Power Effective of VTOL Tail-sitter in Hover Mode

Asst.Prof.Dr.Chinnapat THIPYOPAS

Department of Aerospace Engineering, Faculty of Engineering, Kasetsart University, Bangkok, Thailand

Dec 2023

Abstract

Tail-sitter vertical-takeoff-and-landing concept has been introduced since the 1920s and the studies have been continued in form of unmanned aerial vehicle proposes. This research is proposed as the success of tail-sitter VTOL UAV inspired to enlarge from level of unmanned to manned vehicle. The purposes is to examine the control power and efficiency of the control surface at the trailing edge of tail-sitter VTOL called Elevon (the specific-designed control surface that can perform control like both elevator and aileron). This study focuses on only two significant phases of aircraft mission that are hovering and landing. Size of control surface or elevon in the test are 16.7%, 33.3%, and 50% of wing chord. 3 positions of propeller vary from 10 to 30%C is investigated. The propeller size of 13, 15, and 17inch is powered by electric motor. The elevon could provide control power differently in each scenario due to the differences in thrust power, wind condition. The research is based on wind tunnel testing with the dedicated model to investigate the effect of each relevant parameters. The analysis of data collection from the test turned into the optimal or best configuration that provide maximum control power. The results show the sizing of propeller 15inch and 33.3%C control surface gives the highest pitching moment. When test with the wind coming from the trailing edge represent the landing phase of tail-sitter UAV, the pitching moment can be reduced up to 50% during landing phase.

Keywords: Vertical Takeoff and Landing, VTOL, Tail-sitter, Elevon

Table of Contents

Introduction and Motivation

Now, Unmanned Air Vehicle or UAV have been developed and widely used in many applications. Fixed wing type platform has its advantage in terms of low energy consumption. It uses aerodynamic lift force generated by wing to fly therefore this type of UAV cannot stationarily hover over an interesting target and of course that it needs an area for take-off and landing. Rotary wing platform UAV creates a lift force to fly by rotating the wing or propeller (rotor), so this type of UAV can take-off and land vertically as well as can hover over target. However, it used a lot of energy to rotates the rotor to gaining enough lift force. Both fixed wing and rotary wing type have their limitations in particularly a complex mission or area. The vertical take-off and landing (VTOL) platform then becomes very attractive and very popular since it can take-off and land in a confined area and has an acceptable flight speed and endurance due to its low power consumption compared to a rotary wing UAV. It is a very hot topic for UAV developers around the world. A lot of research have been published [1-5]. There are several VTOL platforms existing today and it can be categorized as following:

Combine-propulsion Type.

This type of VTOL is made by directly combining a set of rotors (like a multi rotor drone) to a fixed wing UAV, either conventional aircraft or tailless aircraft as shown in Fig. 1. The set of rotors is performing during take-off and landing while a propeller of aircraft creates thrust to make the aircraft move forward in the air. The main drawback of this combine-propulsion type is the weight and drag force from the set of rotors during the forward flight phase. Nevertheless, since the propulsions of vertical flight and of forward flight are definitely separated, an optimized engine or motor and propeller for both hovering propulsions set and flying forward propulsion set can be selected.

Helvetis – Jabali VTOL

https://helvetis.com/vtol-uav-isr/

FDG30 Mako Shark

https://www.unmannedsystemstechnology.com/2022/04/6-hour-endurance-electric-vtol-uav-for-mapping-survey-surveillance/

Figure 1: Combine-Propulsion VTOL UAVs

Tiltrotor and Tilt-Wing Type

To solve the disadvantage of a combine-propulsion type VTOL, tiltrotor and tilt-wing are developed. In these types of VTOL, the same propulsion set is used for both flight phases, hovering and forward. A servo or actuator and a tilt mechanism rotate the propulsion set. No extra drag is occurring anymore during the forward flight. However, there is a weight from tilt mechanism and actuator for tilting as well as normal fix-pitch propeller can be optimized for all flight phases. Because the transition between hovering and forward flight is performed by the tilt mechanism, another main issue is the reliability of all these parts. Some examples of tiltrotor and tilt-wing UAV are illustrated in Fix. 2.

Bell Eagle Eye Tiltrotor UAV

https://www.flightglobal.com/new-search-for-vtol-uavs-may-resurrect-bell-tiltrotor/119404.article

Aero2

https://www.unmannedsystemstechnology.com/2023/06/dufour-reveals-final-aero2-design-for-tilt-wing-drone/

Figure 2: Tilt-Rotor, Tilt-Wing VTOL UAVs

Tail-Sitter Type

To eliminate all the weak points of previous VTOL configurations, a combine-propulsion type, a tiltrotor type, and a tilt-wing type, a tail-sitter UAV have been investigated. In this configuration, there is no extra weight of mechanism and non-used part for all flight conditions, and there is no extra critical moving part. So, this configuration is very interesting for future development. The tail-sitter VTOL is one of the VTOL that can perform both limited-space airborne and fixed-wing forward flight in one configuration. This research focuses on the tail-sitter concept as it could provide greater value of power efficiency compared to the multirotor.

In 2007, the tail-sitter mini UAVs first demonstrated at IMAV2007 by the VertiGo (ENSAE-SupAero) and MiniVertiGo (ENSAE-SupAero and University of Arizona, co-research granted by AFRL). Both UAVs are co-axial rotor tail-sitter platform control. SupAero had continued developed the VTOL UAV with the tandem propeller configuration and won the IMAV2009 flight competition in Pensacola, FL [6-8]. In 2012 Roll&Fly, the Air and Air Micro Air Vehicle which is the MAV with a capability of moving on the ground and climbing along the wall and ceiling, was officially patented. The tail-sitter concept has been interested in development by many researchers not popular as other configurations due to the challenge of transition control phase and the difficulty in hovering and landing phase. Fig.3 presents WingtraOne and Vetal UAV which is a good example of commercial UAV on the market.

WingtraOne

https://wingtra.com/mapping-drone-wingtraone/vtol-drone/

Vetal VTOL UAV

https://www.hiveground.com/vetal/

Figure 3: Wingtra One and Vetal Tail-Sitter UAV

https://www.researchgate.net/figure/Current-micro-air-vehicles-a-Mini-Vertigo-b-MAVion-and-c-Disk-wing-aircraft_fig6_301902109

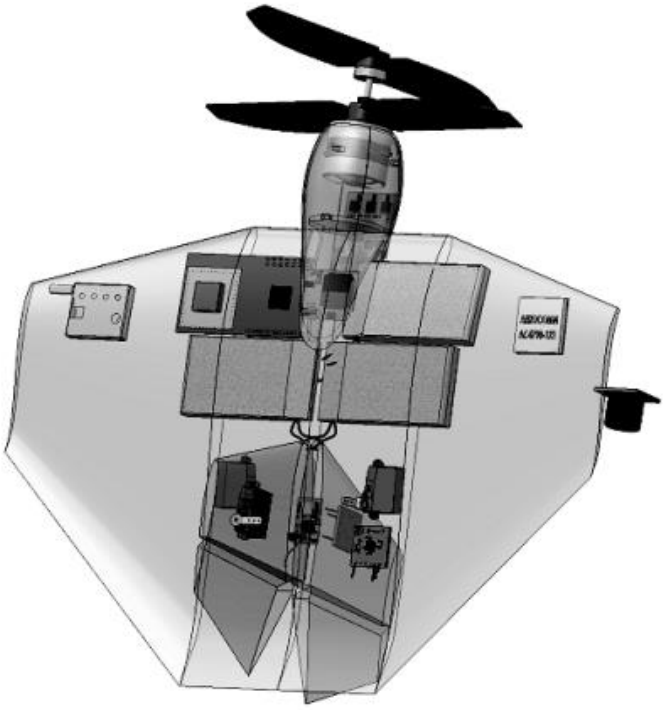

https://journals.sagepub.com/doi/pdf/10.1260/1756-8293.2.2.69

Figure 4: MiniVertigo Tail-Sitter UAV

How does it work; Tail-Sitter UAV

A tail-sitter UAV looks like a normal aircraft with a pair of motor-propellers. Unlike other VTOL UAVs which has at least 4 sets of propulsive system, tail-sitter UAV concept requires just 2 motor-propellers to encounter each propeller torque while it uses benefit of flow induced by propeller through the control surfaces to control the aircraft as commonly used for the fixed wing aircraft. The propeller can be either in tandem as a Wingtra One or in co-axial arrangement as used by MiniVertiGo UAV shown in Fig. 4. Flight profile of a tail-sitter VTOL UAV consists of 3 phases including a) horizontal forward flight, b) vertical take-off, vertical landing, and hover flight, and c) a transition flight from vertical to horizontal and vice versa.

For forward flight, tail-sitter UAV has the same principle of normal fixed wing type aircraft to fly (Fig.5). Thrust from the propeller introduces forward movement of vehicle counter the drag force then wing generates lift force and finally the vehicle can fly. Control surfaces on the wing and/or tail are used for controlling the aircraft including roll, pitch, and yaw via aileron, elevator, and rudder, respectively. In addition, differential rotating speed of propellers can be applied and used for controlling the aircraft in certain axis as well depending on the configuration and the arrangement of propellers installation.

Figure 5: Attitude Control of Tail-Sitter in Horizontal Mode (Forward Flight)

In vertical mode, as illustrated in Fig. 6, tail-sitter UAV can hover by thrust or lift force generated by both large propellers. Due to a pair of propellers, torque of propeller has canceled each other, tail-sitter can stationarily fly. Aircraft can climb up by introducing more thrust and descent down by reducing throttle. To control a rotation of aircraft, tail-sitter uses the benefit from

propwash induced flow through the control surface located on the trailing edge generating aerodynamic force and moment.

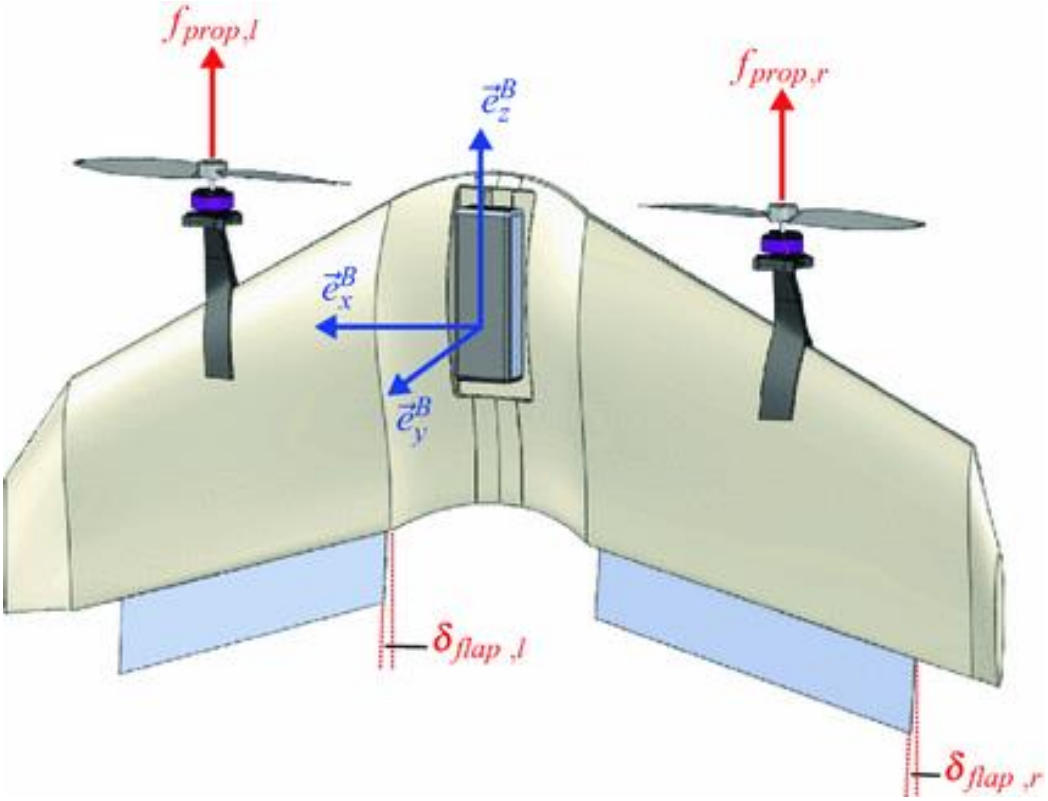

https://link.springer.com/chapter/10.1007/978-3-319-51532-8_2

Figure 6: Tail-Sitter UAV in Vertical Mode (Hover Flight)

Finally, for the transition flight, the tail-sitter changes from vertical mode to horizontal mode by controlling the pitch of aircraft via an elevator in propwash induced flow and proper increase throttle to increasing speed of vehicle. This phase is also one of the critical phases of tail sitter UAV too. An efficient automatic control theory must be considered and applied if, especially, the nice and smooth transition flight is required. The control law and system of tail-sitter platform is an interesting topic for researchers to make it fly smoothly. A lot of work have been done [9-13].

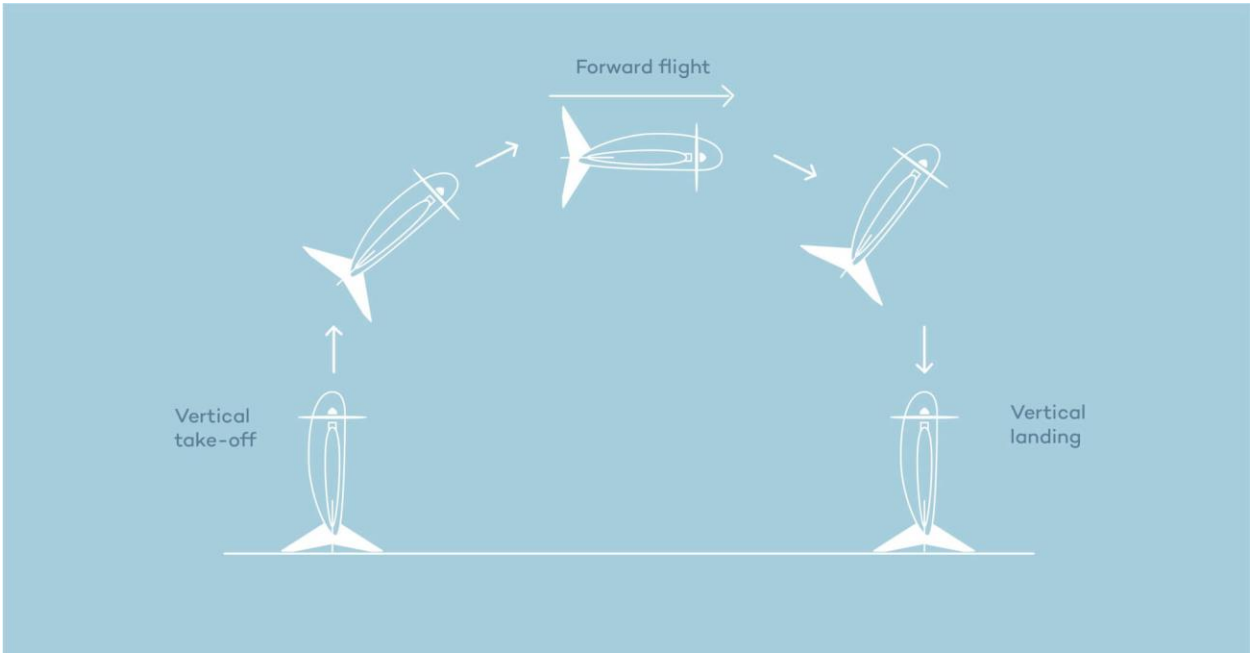

Figure 7: Transition of Tail-Sitter UAV

The challenge of Tail-Sitter UAV

As described above, tail-sitter used a flow behind its propeller pass through wing and control surface to create moment and control attitude of aircraft. Let use conventional body frame X,Y,Z corresponds to the axis along the fuselage or body (X), the axis through the right wing (Y), and the axis downward under the body (Z). For a tandem propeller tail-sitter, illustrated in Fig.8, nose down pitch motion, aircraft rotate about Y axis, can be performed when both left and right elevons deflect downward while it will be nose up when elevons deflect upward. To rotate along X axis, it can be done by deflecting left and right elevon in opposite direction. In this case of tandem propeller, the rotation along the Z axis can be done by applying differential thrust on right and left motor-propeller. It is noticeable that yaw motion is directly achieved by applying different of thrusts while the other two motions are due to an aerodynamic force on the control surface from the flow behind propellers. In addition, in vertical mode, a large wing is normal to lateral wind, of course it is

high drag, resulting in a difficulty to control the position during landing. This is one of the most critical disadvantages of tail-sitter UAV.

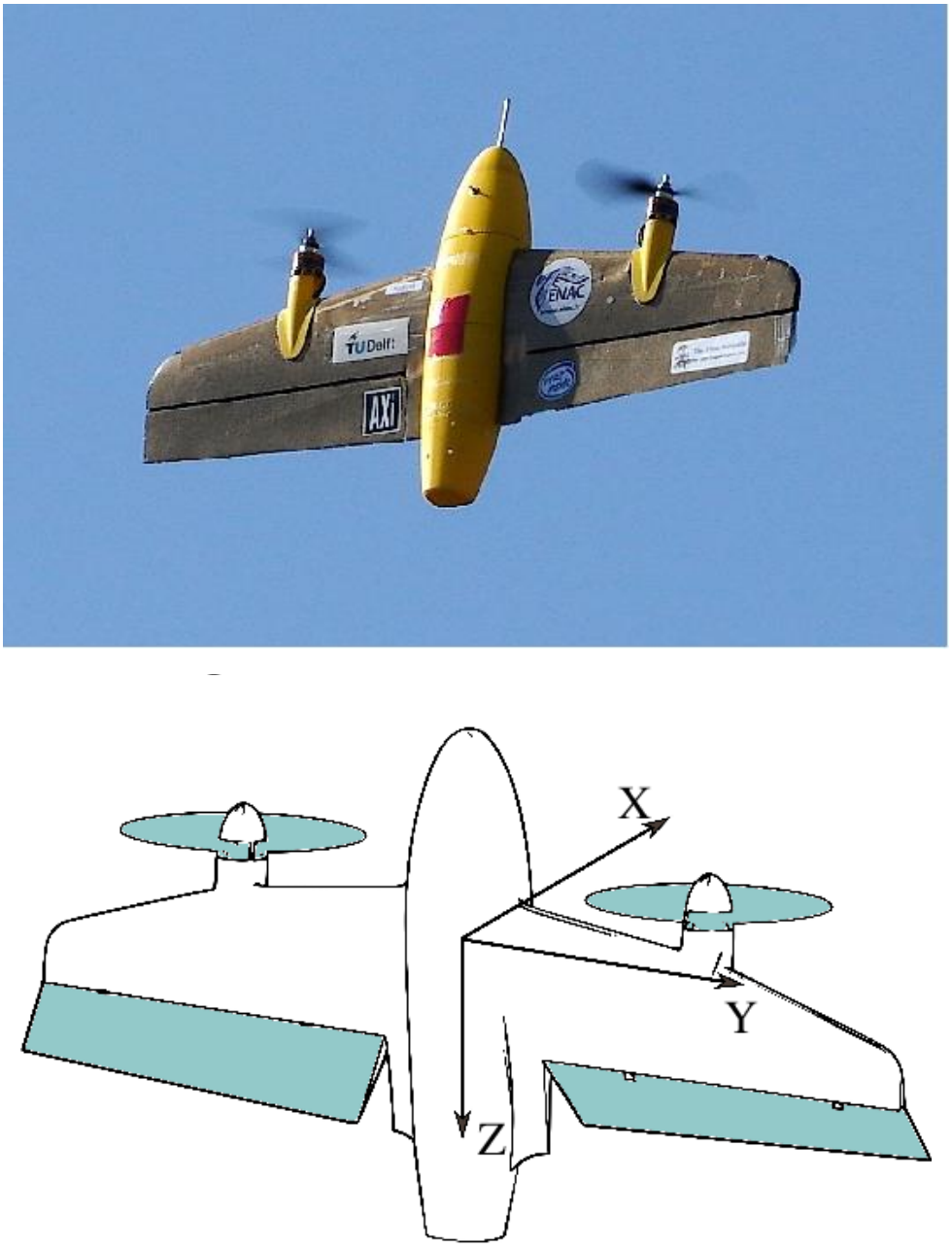

Figure 8: Control of Tail-Sitter in Vertical Mode

https://www.semanticscholar.org/paper/Incremental-control-and-guidance-of-hybrid-aircraft-Smeur-Bronz/6be6231995b902e74dd1691fbaf758f37e3f0d7b

To reduce the difficulty during the vertical mode, in particular hover in windy environments, many researchers and designers invent few solutions.

- An engineering team from ENAC proposed a concept and control algorithm of rotate the body parallel to the wind as shown in Fig. 9. This concept successfully eliminates a high drag force on the wing. Nevertheless, it may introduce an asymmetry of control power on left and right control surface as illustrated in Fig. 10.

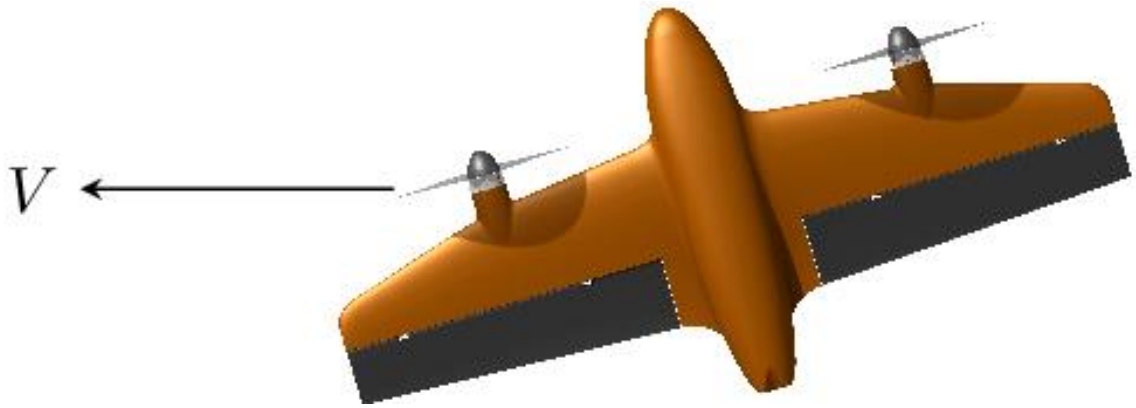

Figure 9:

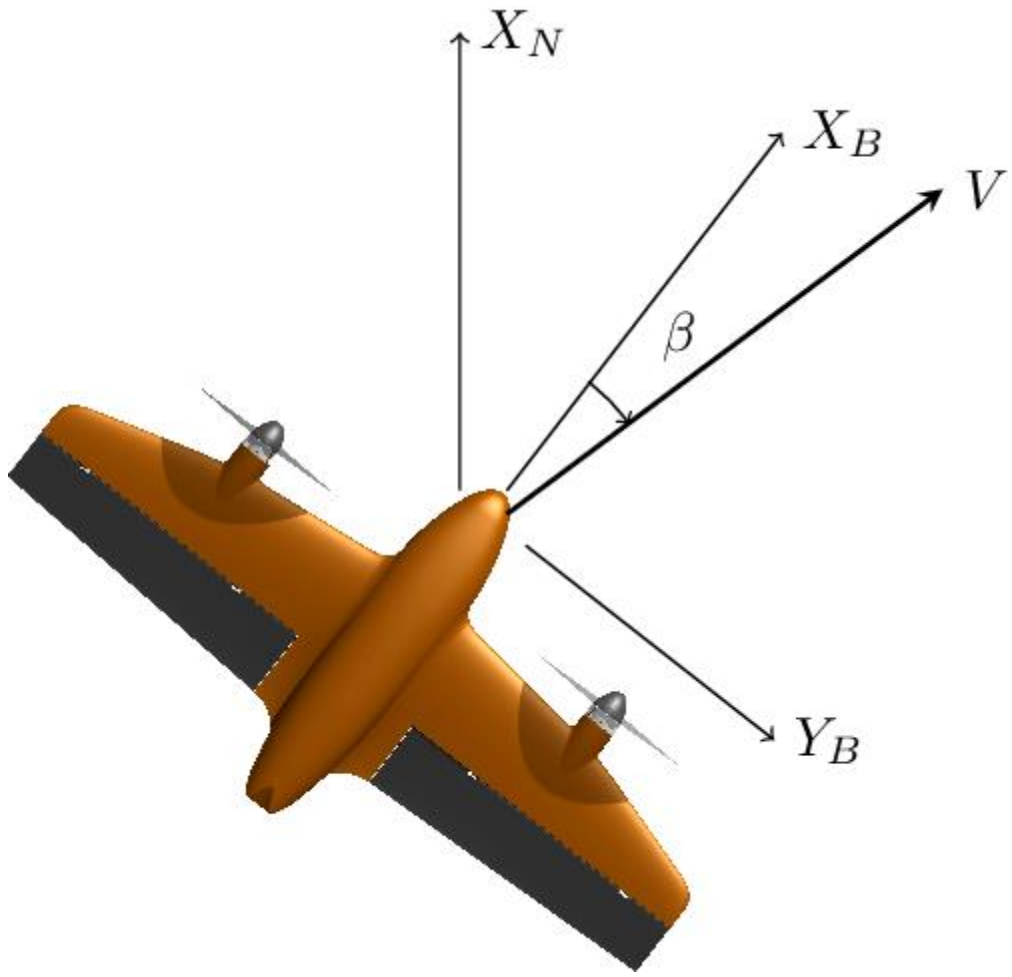

Figure 10:

- In 2019 and 2020, a student team from Kasetsart University built a tail-sitter UAV, named Nontri, and participated and won in METU VTOL Competition organized at Ankera, Turkey, and in AAVC (Autonomous Aerial Vehicle Challenge) in Thailand. To enhance the controllability during the vertical mode, they used thrust vectoring concept by install the motors with a tilt mechanism closed to concept of [14]. For a few usages and operates by a good knowledge, as an engineering team a competition, it results very well. However, after several flights the tilt mechanism and part are need more maintenance. Moreover, the damage on the tilting servo often occurred. And this is back to the disadvantage of tiltrotor and tilt-wing VTOL UAV platform.

Figure 11: Nontri UAV

- Quad propeller concept is another solution which can be found both in biplane and monoplane wing tail-sitter UAV. The vehicle is now able to direct controlled by adjust the thrust of 4 rotors, can be either with or without control surface in horizontal forward flight. This concept performs very well and applied in the Xeva, an eVTOL with human onboard. By the way, it seems over design for using 4 motors in horizontal level flight phase. [15-16]

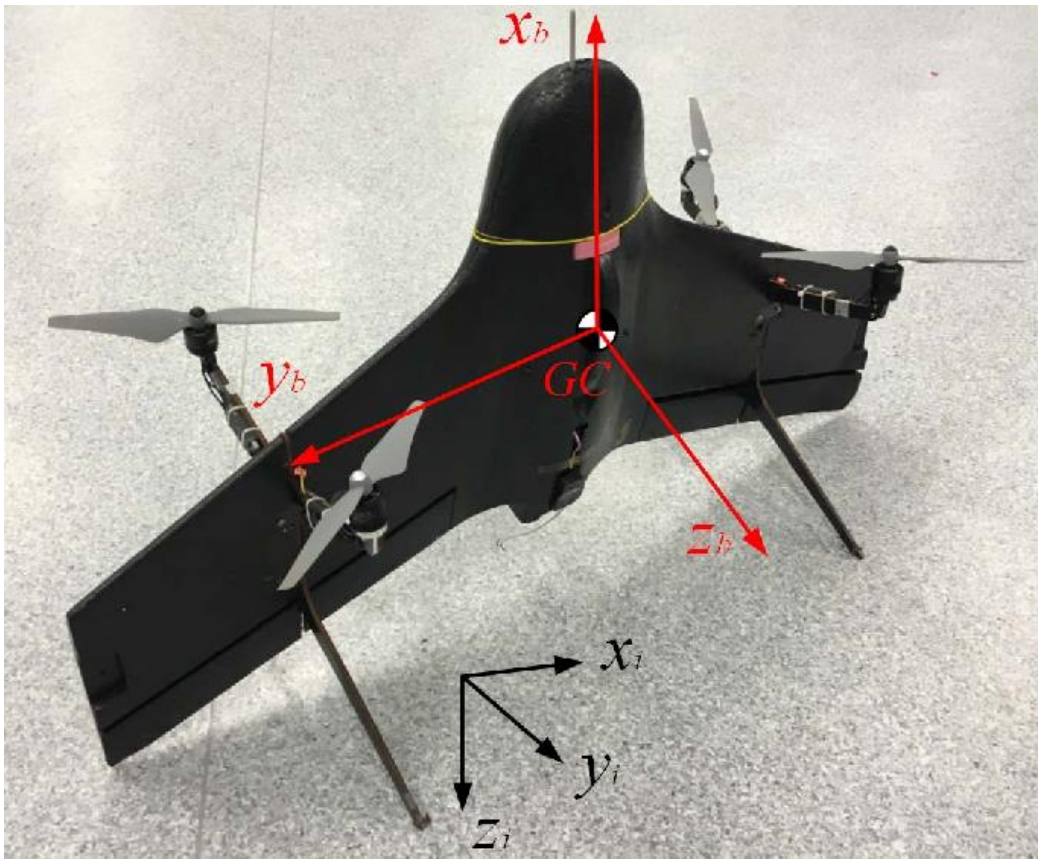

Figure 12: A Quad Rotor Tail-Sitter UAV

https://www.semanticscholar.org/paper/Design-and-implementation-of-a-quadrotor-VTOL-UAV-Lyu-Gu/d587481492518ad331c5b622e81482abb993ad75

Research Objectives

Although, few solutions as detailed above are available, it is still interesting and challenging for researcher if the most effective control of tail-sitter can be found with a good combination between propeller and control surface installation. Therefore, this research focuses on the finding of suitable control surface and propeller for hovering control of a tail-sitter UAV. The main interesting parameters to be observed are:

- Size of Control Surface: Percentage of control surface size to chord length is used.
- Size of Propeller: this parameter is conducted by non-dimension term of Propeller diameter-to-wingspan ratio.
- Position of Propeller from the Wing Leading Edge: Percentage of control surface size to chord length is used.

And, in addition, the effect of control surface deflection angle and different throttle level are investigated as well. Finally, some of the controllability in landing conditions also be observed.

Methodology

Wing-propeller interaction, especially with a low aspect ratio wing, is a complex problem. In 2017, Chinwicharnam et al studied an aerodynamics interaction of a propeller and a clean wing without control surface by CFD method and compared with experiment conducted in a wind tunnel. Although a CFD simulation gave a good trend of aerodynamic characteristics when compare test result, but the value is still highly disagreed [17-18]. For this research which a deflection of control is added that might introduces more complexity of flow phenomenon. Therefore, experimental method is selected in this first step on the research plan. With the result and data of this experimental test result then can be used for the further next step. Only longitudinal aerodynamic characteristics is interested and conducted for this study, therefore a wing with a single propeller is used. Normal force, axial force, and pitching moment are measured. The detail of experimental and testing facility will be explained in next section. Table 1 and Fig.13 show the investigated parameters conducted in this research.

Table 1 Test Parameter

Parameter	Notation	Value
Size of Control Surface	CS	16.67, 33.33, 50.00 (%C)
Deflection Angle of Control Surface	CA	0, 15, 30 (deg)
Size of Propeller	PS	13, 15, 17 (inch)
Position of Propeller from Leading Edge	PP	10, 20, 30 (%C)
Wind		Wind / No Wind
Throttle	PWM	1200, 1400, … 1800

To complete full experience of 5 parameters above, numerous tests must be conducted. In addition, several step changes of throttle should be performed and collected therefore a lot of tests must be investigated. To reduce the number of tests and because the interest is the parametric sensitivity effect, the design of experiment will be conducted by fix all other parameters while vary

only one interested parameter. Finally, a total of 5 sets of experiments are investigated as detail in this Table.

Table 2 Concept of Test Parameter

	P	C	U	D	V	Interested Parameter
1	Vary	Fix	Fix	Fix	Fix	Propeller to Span
2	Fix	Vary	Fix	Fix	Fix	Control Surface to Chord
3	Fix	Fix	Vary	Fix	Fix	Velocity
4	Fix	Fix	Fix	Vary	Fix	Wind Direction

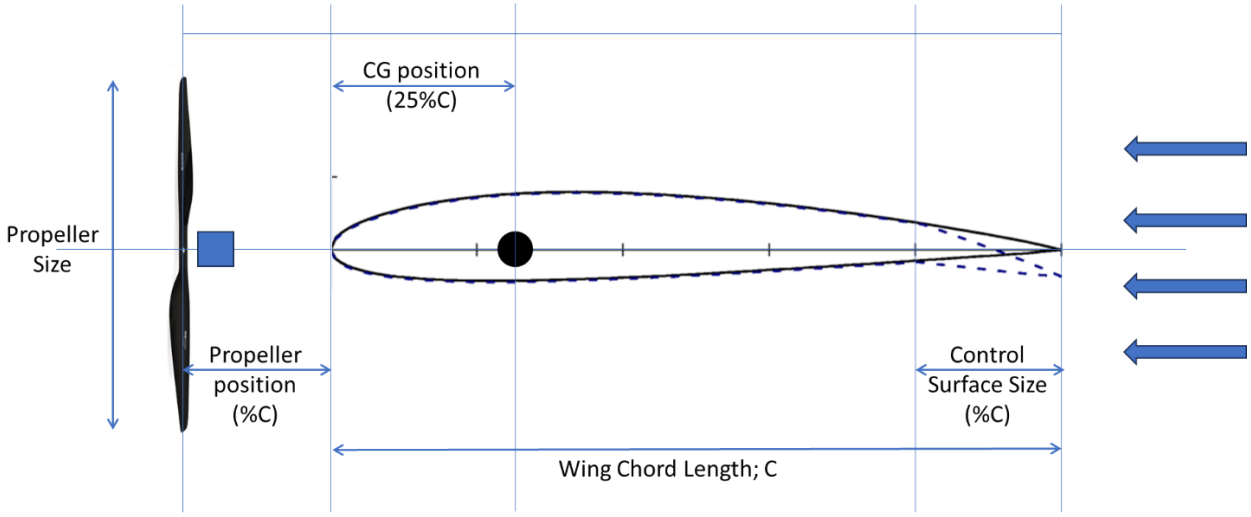

Figure 13: Schematic Diagram of Wing Parameters

Size of Control Surface

Tail-Sitter UAV primary uses the control surface to control its attitude during the vertical hover mode. Therefore, the first parameter focused on this research is of course the size of the control surface. For most tail-sitter UAV is a flying wing platform, a rectangular wing planform seems a good candidate for the basic understanding. For low aspect ratio wing, the aerodynamic center is about at 30 percentage of wing chord, then assume the center of gravity of the UAV is located at 25 percentage of chord, to have a reasonably good longitudinal static stability margin. Consider the force created by deflection of control surface is at about 25 percentage of control surface measure from elevator hinge and the force per area is equal for each control surface size configuration. Hence, the pitching moment generated by the deflection of control surface can estimated by Eq.1. Table 2 presents the pitching moment for each case of control surface size. Due to the moment arm that decreases when increase the size of control surface, the desired pitching moment is not linear enhance with size. From this simple estimation, the control surface size of more than 50 percentage does not provide better pitching moment to control the aircraft. Finally, the size of control surface is then selected and designed by a range of 0 to 50 percentage of wing's chord length.

M = Control Surface Area x Moment Arm from CG to 25% CS (Eq. 1)

Where assume a force created from control surface (CS) is linear function of CS area

Table 2: Estimated Pitching Moment Generated by Varying Control Surface Size

Control Surface's Size	Hinge Location	Distance from CG	Estimated Moment
(%C)	(%C from leading edge)	(%C)	
0	100	75.00	0.00
5	95	71.25	356.25
10	90	67.50	675.00
15	85	63.75	956.25
20	80	60.00	1200.00
25	75	56.25	1406.25
30	70	52.50	1575.00
35	65	48.75	1706.25
40	60	45.00	1800.00
45	55	41.25	1856.25
50	50	37.50	1875.00
55	45	33.75	1856.25
60	40	30.00	1800.00
65	35	26.25	1706.25

Deflection Angle

Normally, the maximum usable deflection of control surface is about +/- 20 degrees and not exceed +/- 30 degrees, so the range of deflect angle between 0- and 30-degrees is performed in this experimental test.

Size of Propeller

For this size of tail sitter UAV, Wingtra One, Vetal, and Nontri, the aircraft's weight is about 3 to 5 kg. Therefore, the size of the propeller, as well as the motor, is selected from the propeller that able to give a thrust of 1.5 to 2.5 kg (half wing).

Propeller's Position from Wing Leading Edge

Motor is one part that has significant weight ratio for the tail-sitter. If the motor propeller is located far from the wing leading edge, the wight or center of gravity balance will become impossible. 10, 20, and 30 percentage of chord from wing leading edge for the propeller installation position is, then, explored in this research.

Experiment Set Up

To conduct the experiment, there are divided into 4 parts: a wing part, a longitudinal measurement part, a wind generator part, and a control and data collection part. A Schematic diagram of experimental set up is presented in Fig. 14. A wing part is vertically installed to a longitudinal measurement part as seen on the right and placed just in front of a wind generator part. A control and data collection part are used for controlling the throttle of motor mounting at wing leading edge and for controlling the wind speed of wind generator. All the data including axial force, normal force, pitching moment of the wing model, and force of motor-propeller. The detail of each part is explained in this section.

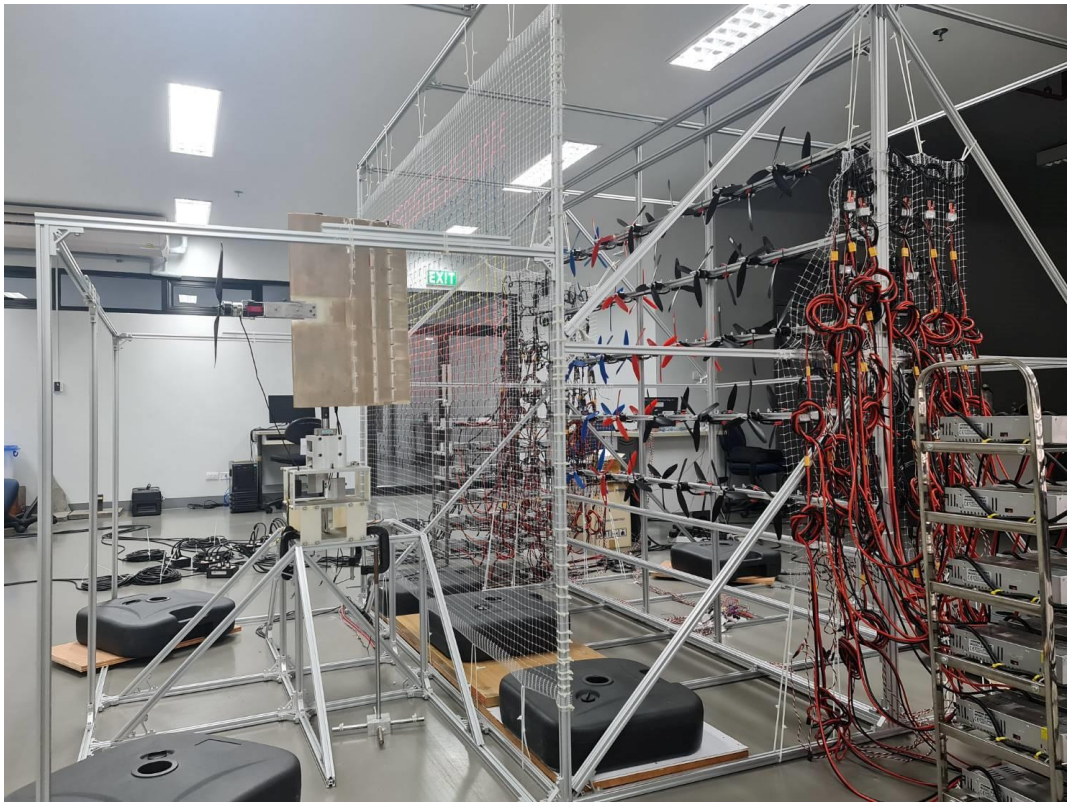

Figure 14: Schematic Diagram of Overall Set Up

Wing Part

The size of the wing is selected by on-the-shelf available well-known tail-sitter UAV, the Wingtra One, which is very close to the Nontri UAV of Kasetsart University and the Vetal UAV of HG Robotics which has a wingspan around 120-130 cm. and wing aspect ratio around 3. A simple rectangular wing with NACA 2412 airfoil is designed. The chord of wing is 45 cm. Wing is first modelled in CAD program including control surface and motor mounting to ensure that everything is correct before manufacture. Fig. 15 presents the CAD model of wing design.

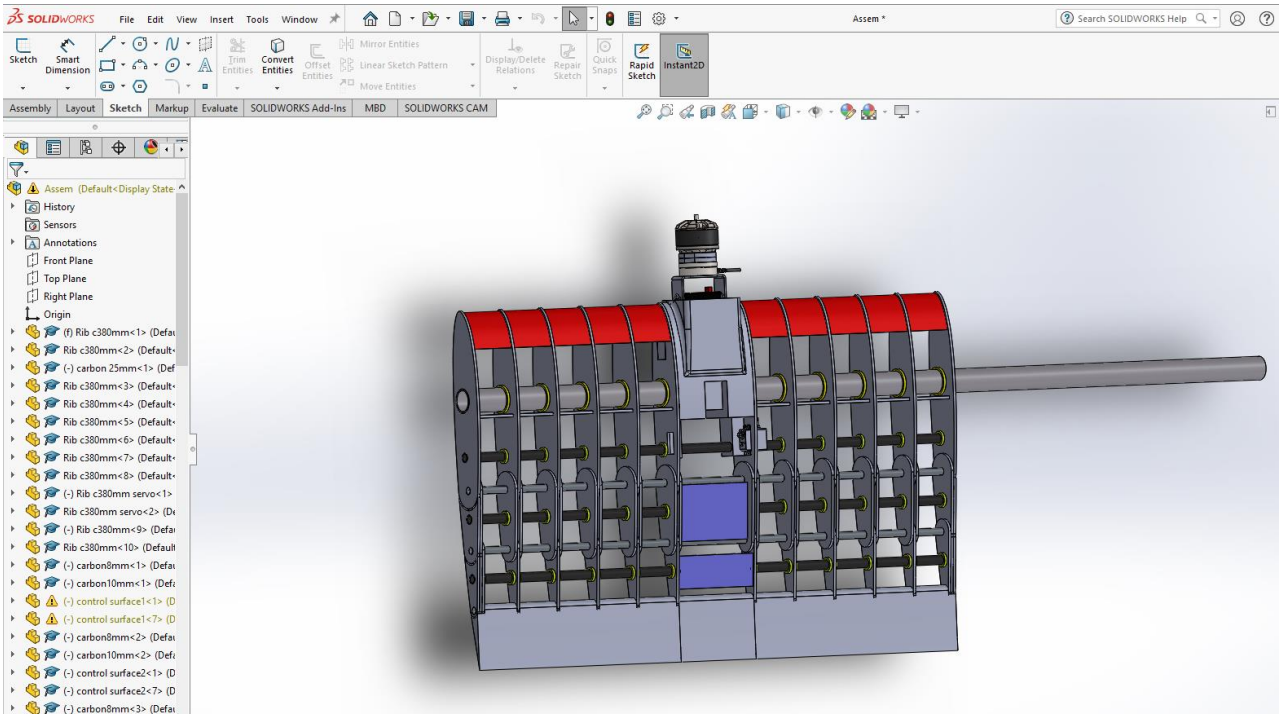

Figure 15: CAD Model of Wing

Once the CAD design is completed, each part was fabricated by CNC machine shown in Fig.16a. Some available part such as a carbon fiber tube can be found on the market. Finally, wing model was assembled as shown in Fig.16b. A set of motor mounting with different length (10,20, and 30%Chord) is prepared and able to change during the testing.

a- Part Manufacturing

b- Wing Assembly

Figure 16: Wing model

To well understand the interaction force from propeller on the wing, ATI Mini40 force transducer is placed between motor and mounting. This is to observe the force and torque of motor-propeller and then will be subtract from the total force measure by longitudinal measurement part to obtain aerodynamic force and moment of wing. The final wing part which consists of wing, control surface, motor mounting, force transducer, and motor-propeller is presented in Fig. 17.

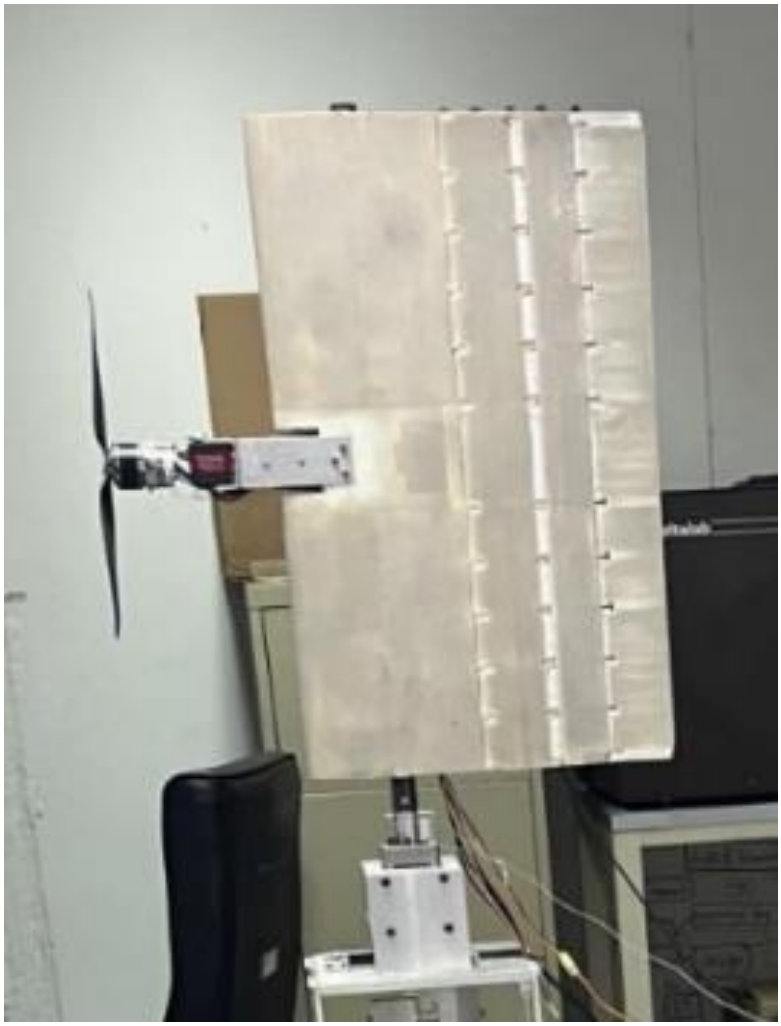

Figure 17: Wing Part (Wing, Control surface, motor mounting, transducer, and motor-propeller)

Longitudinal Measurement Part

In-house designed 3-component force torque balance is used in this study. It combines 3 single-point load cell installed in different location to measure axial force, normal force, and pitching moment of wing model as illustrated in Fig.18. This means the axial force obtained will be represented as the net lift force of the model equivalent to the mass of vehicle since we are considered and tested in vertical mode. While the pitching moment measured by this force balance directly represents the pitching moment around the center of gravity (CG) of aircraft because the

axis of wing model made by 25mm-diameter carbon tube is located at 25% of wing chord length which assumed to be the CG. A known mass range of 0 grams to 1.5 kilograms is used for calibration of each force component. All signals are then sent to the NI Compact DAQ 9237 for data collection. According to the structure of this force balance, the accuracy of measurement depends on the stiffness of the connector plates.

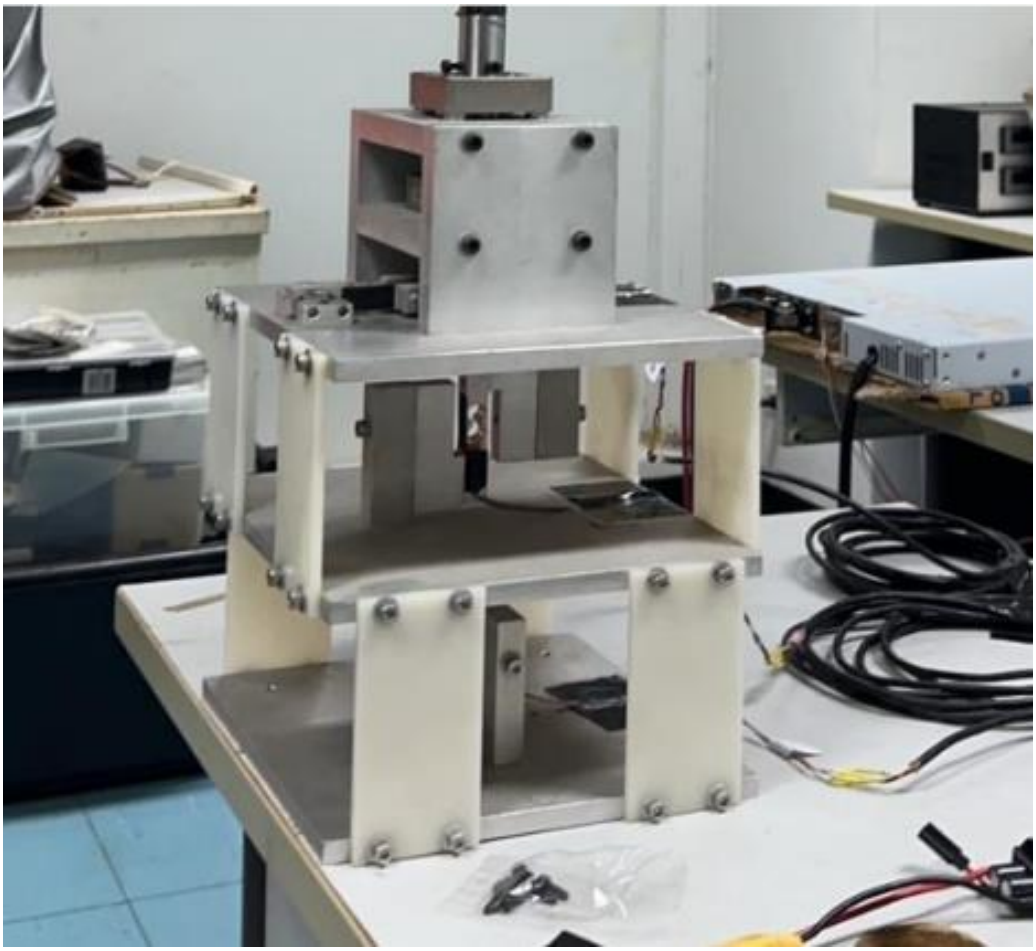

Figure 18: 3-Component Force Balance

Wind Generator Part

In the original plan of this project, a low-speed wind tunnel test section size of 1m x 1m x 3m will be used for this research (Fig.19a). It is located at Sriracha Campus which is approximately 2 hours-drive from Bangkok. Unfortunately, the building of this wind tunnel had to be renovated all the building so the wind tunnel had to be shuttled down for a year (around October 2022 to August 2023). Therefore, two alternative solutions were made available.

- Ask for the support from a Low-Speed Wind Tunnel from Thai Royal Airforce Academy School (Fig.19b). Unluckily, they have a big plan to relocate the whole school from Bangkok to another province. So, it is not possible.

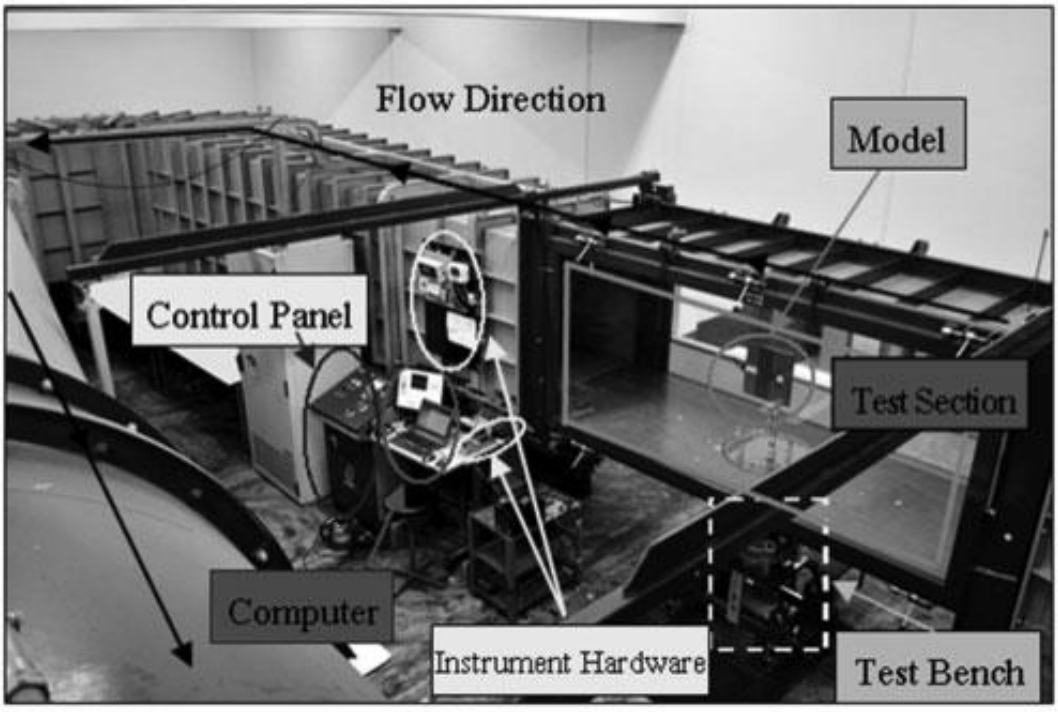

a- Kasetsart Wind Tunnel at Sriracha Campus

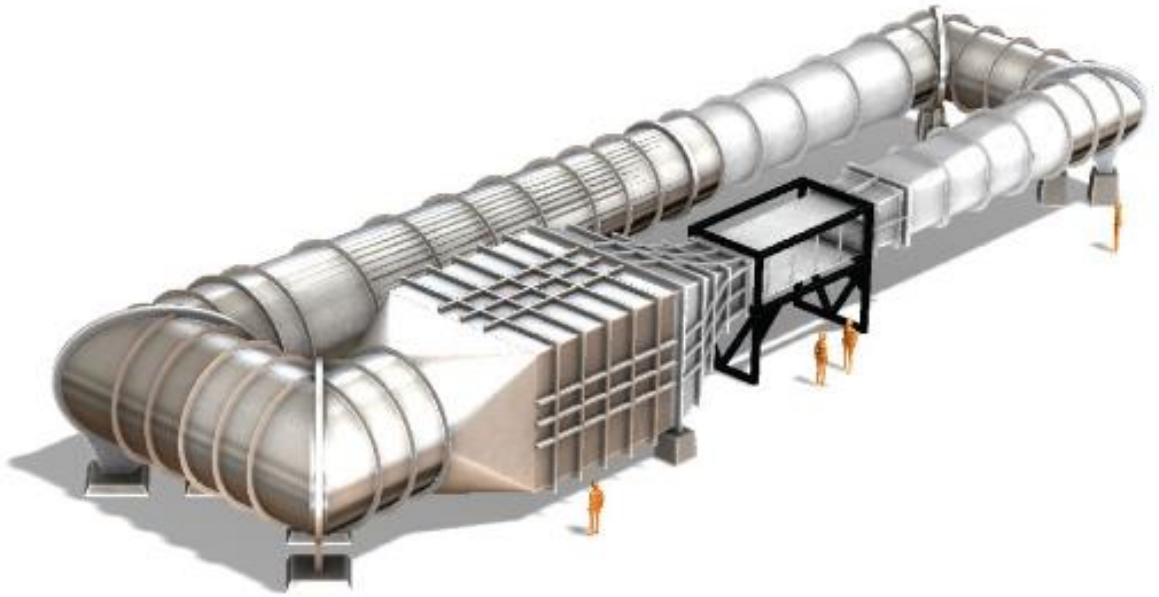

b- Wind Tunnel of Thai Royal Airforce Academy School

Figure 19: TRAF Wind Tunnel

https://kinetics.co.th/projects/royal-thai-air-force-aerodynamics-research-wind-tunnel-facility/

- Design and build new Wind Generator. Nowadays, Wind Shape (Fig.20) propose a concept of wind generator consist of an array of small ventilator. And it is already used by some institutes research on the drone. The advantage of this concept is that the speed at each position can be adjusted, therefore it is used for testing the drone flying in more real situations.

Figure 20: WindShape

https://windshape.com/

Finally, there are very limit of choice then the second option of build new Wind Generator is selected. In addition, even the wind variation is not the scope of this project, but the wind generator will be very useful for the next research project.

To reduce the swirling flow of single propeller or fan, a coaxial propeller is chosen. An available propeller set can be found in Thailand seem to be a motor-propeller for RC. Therefore, a series of brushless motor size of 2814 1300kV with the 3-blade propeller size of 10x4.5 is selected. The rotational speed is then controlled via 50 Amp ESC (electronic speed controller). This is selected from the maximum desired wind speed of at least 10m/s which calculated by propeller momentum theory. To flexibility in adjustment of the position of each motor-propeller, the structure is made with aluminum extrusion profile. A quick Finite Element Analysis is performed to unsure the rigidity of the structure as well as to understand a vibration which might be damaging to wind generator. The details of design, build, and test of wind generator are in an Annex B. After construction of the wind generator finished, wind speed is observed by low-cost hot wire anemometer and a tuft method on the net installed on a plan behind a propeller's plan. From the tuft on the net, and velocity observations, the outcoming flow on the location of the wing installation is quite uniform and acceptable for the test. Note that this construction part and validation of wind test mainly done by 3 intern-students from France during May 2023.

Figure 21: Wind Generator

Control and Data Collection Part

There are 2 subparts in Control and Data Collection Part: a) Subpart A - wing model control and measurement and b) Subpart B - wind generator control and measurement as shown in Fig.14. The control and data collection is done via NI Compact Daq and Arduino board as shown in Fig. 22.

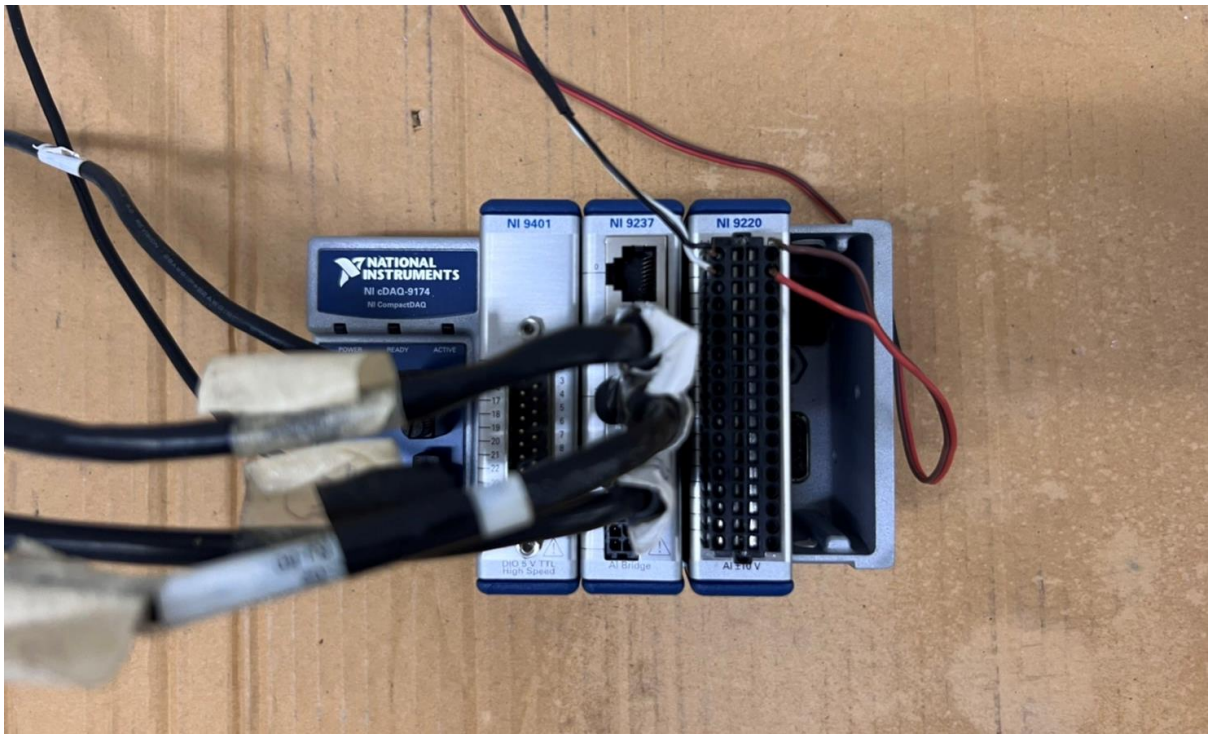

Figure 22: Data Acquisition System (NI Compact DAQ and Arduino Board)

Subpart A involves with the wing model part and the longitudinal measurement part. Therefore, the control parameter includes the control of throttle. Although the adjustment of control surface deflection angle is originally designed to be control by the PWM signal, it is now adjusted manually by the operator due to the high friction of hinge and for precision of deflect angle. The data collection for the subpart A are:

- All 3 longitudinal aerodynamic force and moment from the longitudinal measurement which measure a) axial force or resultant lift force (the model in vertical mode), b) normal force or lateral force, and pitching moment around the CG of wing model.

- Thrust of motor-propeller from the ATI MINI 40 transducer. Since only longitudinal characteristics is focused, only thrust force from the Z-axis of transducer is collected via NI USB 6220.
- Electric power from the DC power supply. The electric voltage and the electric current consumed by the motor-propeller are measured.

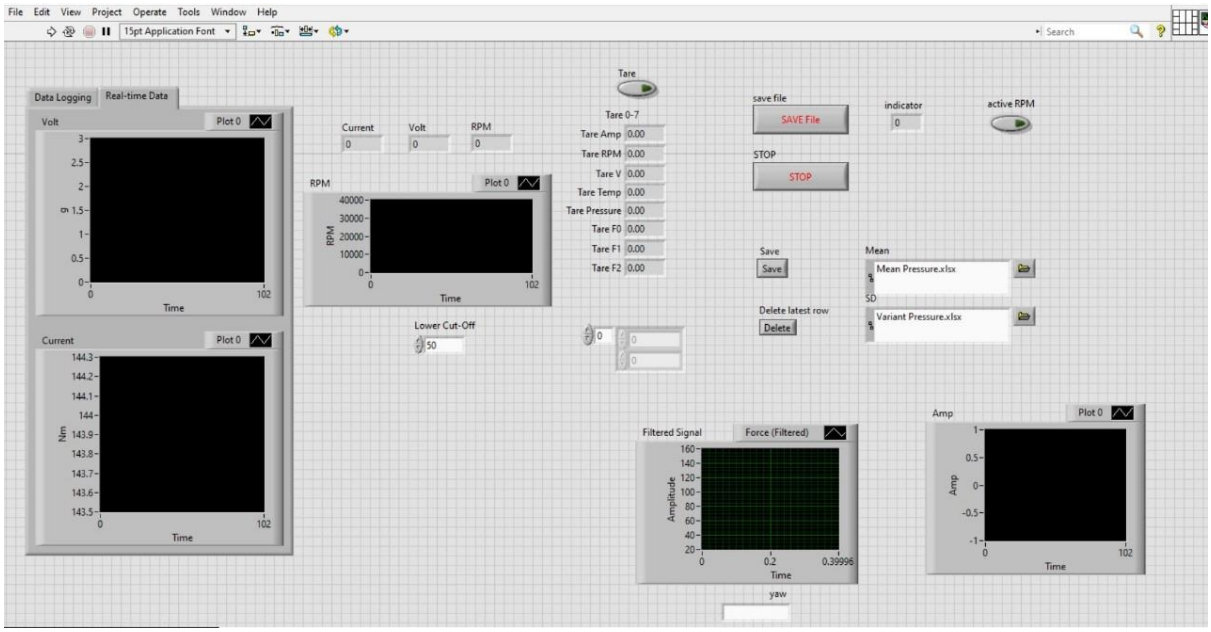

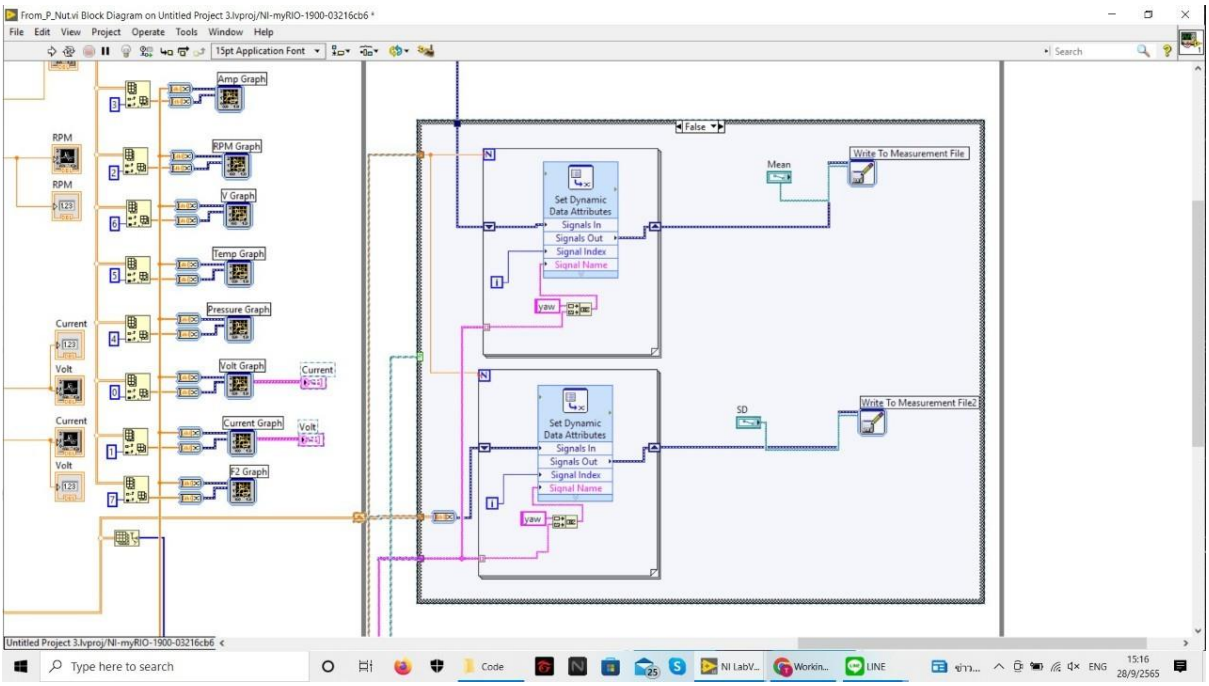

Figure 23: Longitudinal Measurement Data Interface

Figure 24: ATI Mini 40 Data Interface

Figure 25: High Power DC Power Supply

For all measurement, the average value from 1000 sample data and the standard deviation are collected from the measurement and then save into excel csv format. Then is used for the data processing and analysis of result in the next step.

Subpart B is used for wind generator part. All the 60 motors of wind generator are desired to rotate at identical speed to obtaining most uniform flow. Wind speed is observed by hotwire anemometer in function of input command or control signal.

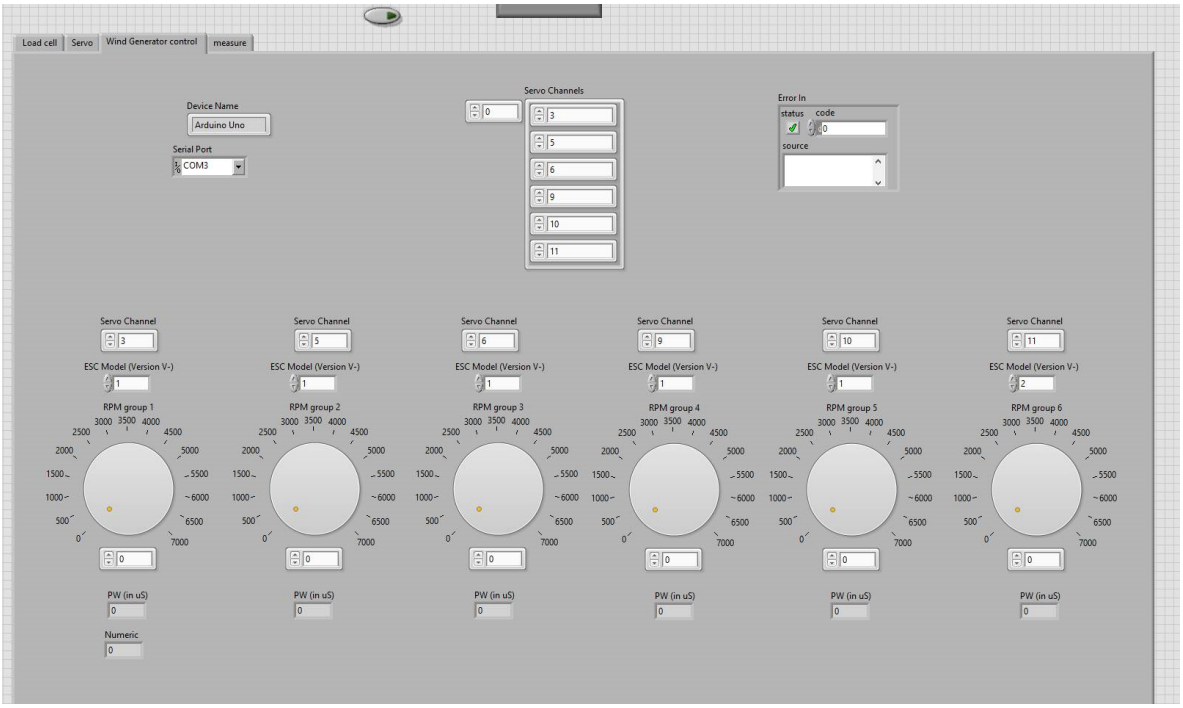

Figure 26: Wind Generator Control Interface

Total number of small fan is 60 units, place into 30 positions in the plan. Then they are divided into 6 groups in order to control the speed in the future project. Nevertheless, all 60 fans are controlled to have same rotational speed in this test.

Calibration

As mentioned above, the loadcell is calibrated by applying a known mass for each direction including all three components of longitudinal measurement part an as well as the thrust component at ATI Mini 40 transducer. The calibration set up and the result are illustrated in Fig. 27-28.

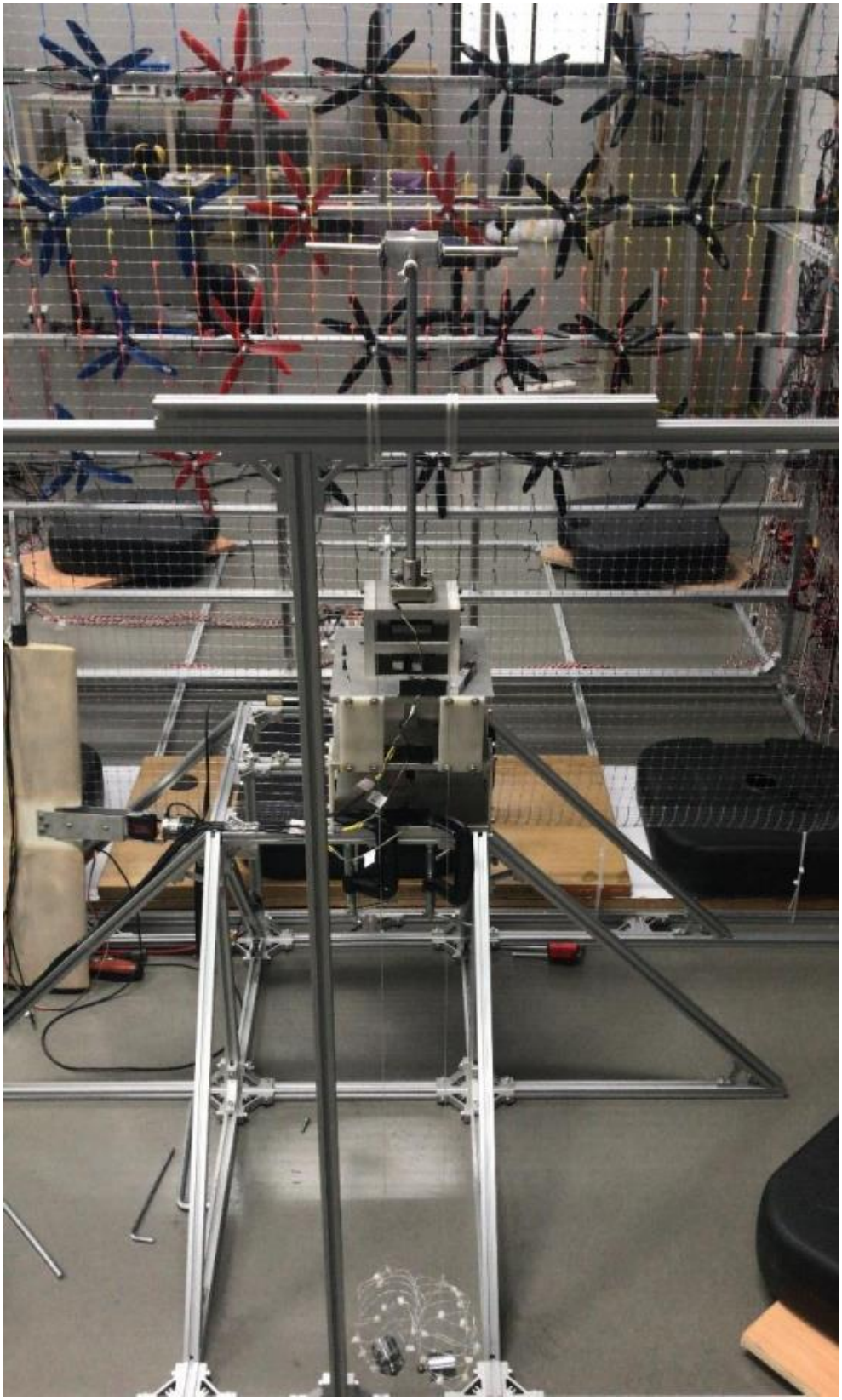

Figure 27: Calibration Set-Up

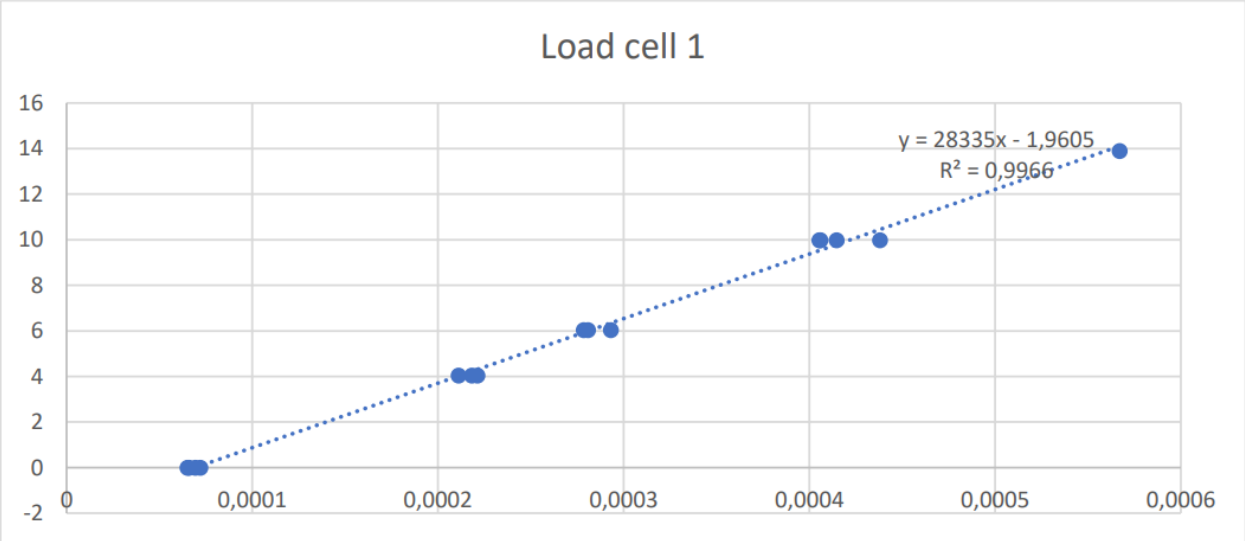

Figure 28: Example of Calibration Result

Repeatability of Measurement

To ensure the experimental set-up, the procedure, and the measurement, repeatability test is performed. One configuration of wing model is selected then repeat the test for 3 times, the result is plotted and presented in Fig.29. All three results are very good agreement each other. This can confirm the reliability of this experiment.

Figure 29: Repeatability Result of Experiment

Parameter of Testing

The diagram of force and moment measured obtained from this experiment is illustrated in Fig.30. It consists of 3 longitudinal forces - moment of the whole wing model and thrust of motor-propeller.

Where:

Thrust is measured by ATI MINI40 Force-Torque Transducer

Lift is measured by the longitudinal Loadcell No. 2

Horizontal Force is measured by the longitudinal Loadcell No. 1

Pitching Moment is measured by the longitudinal Loadcell No. 3

Then

Propwash Drag can be found by Thrust and Lift

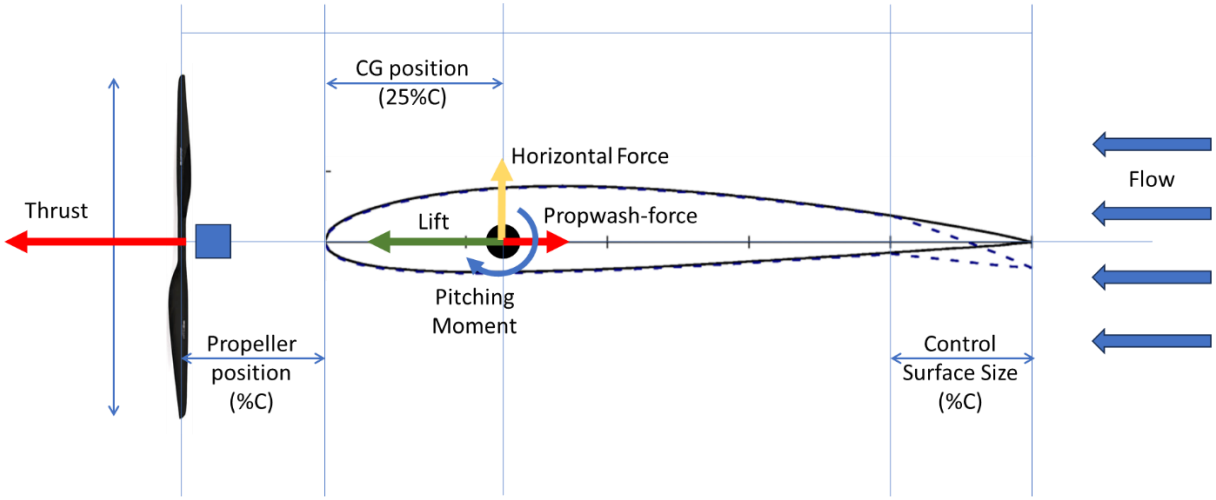

Figure 30: Force and Moment Diagram of Testing

Results and Discussion

There is the test without wind represent the vertical hovering condition of the tail sitter UAV and the test with wind coming from the trailing edge represent the tail sitter UAV during landing phase which is one of the most critical for tail-sitter UAV. Both investigation's results are presented in this section.

No Wind Condition

There are mainly 4 parameters investigated in this research: Control Surface Size, Deflection of Control Surface, Propeller Size, and Propeller Position. There are 3 interval steps for each parameter. Total 4^3 configurations are investigated for no wind condition. In the experiment, the throttle of all tested configuration is controlled by identical PWM signal (1000 to 1800 PWM). All test results are plotted and shown in Fig.31.

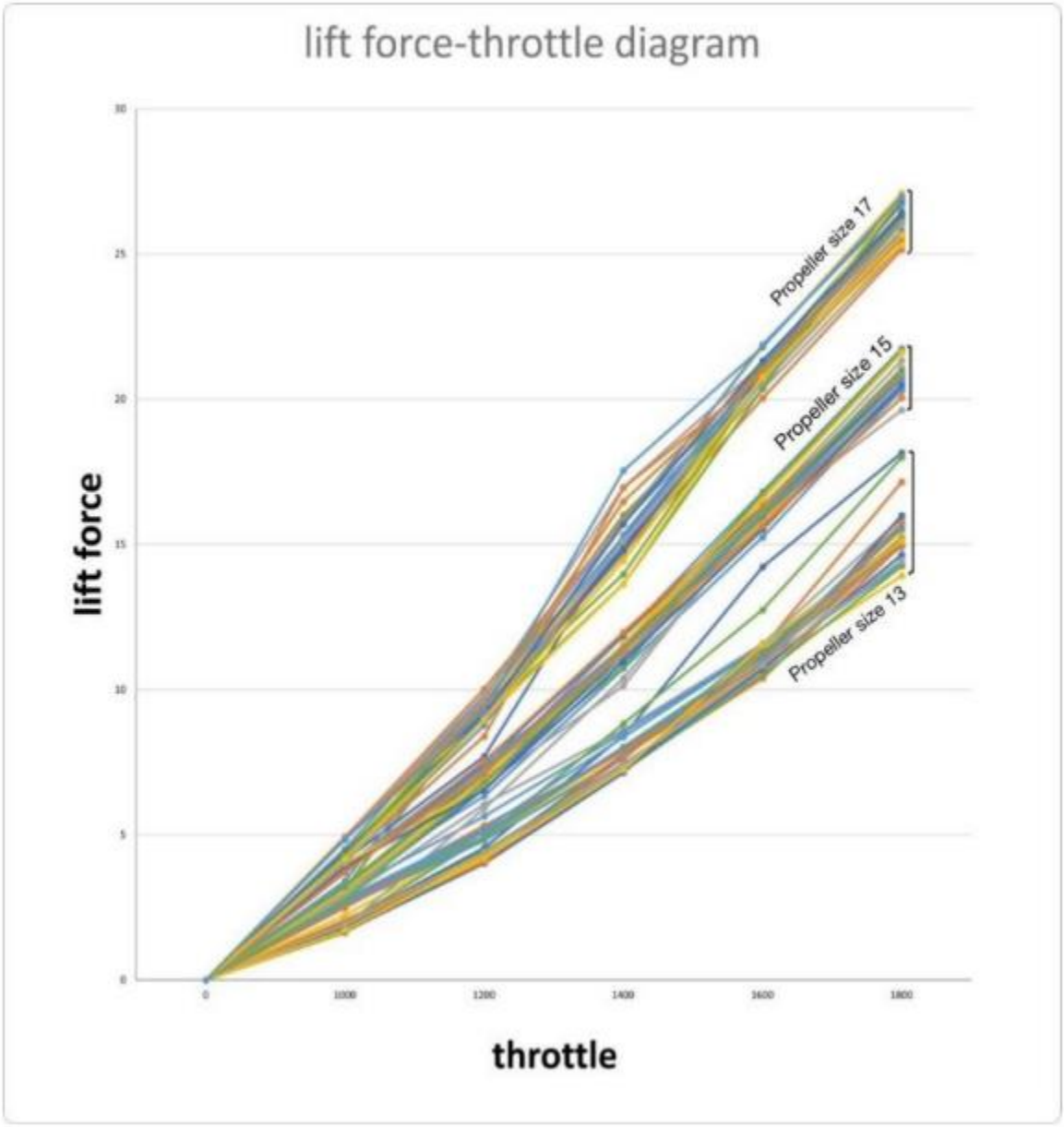

Figure 31: Lift Force versus Throttle (PWM signal)

It clears that for the same PWM input, larger propeller size gives higher lift force. Lift force of all configurations with the same propeller size at the given throttle (same PWM) is slightly close. However, the main interesting result in this research is to find the most effective in control power or pitching moment produced in vertical mode. Although for same propeller size, the lift force is quite similar and close, but it is exact identic lift, it is not right to compare the pitching moment by plotting with the throttle. Therefore, instead of plotting the result in function of throttle (PWM signal), the plot

of lift force from the load cell no.2 presents more reality in vertical hovering condition. The effects of elevon control power for each parameter are detailed and discussed in this section.

Control Surface Deflection Angle

Figure 32 illustrated the pitching moment of wing model with the 15-inch propeller installed at 30%C from the wing leading edge. As expected, pitching moment is enhanced by increasing of deflection angle.

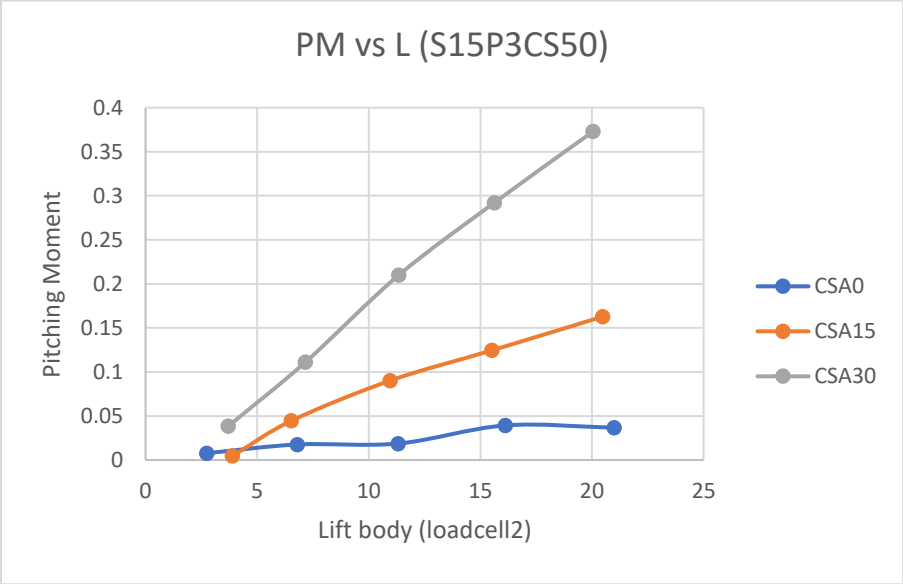

a) Propeller 15inch located at 30%C from wing leading edge with the elevon size of 50%C.

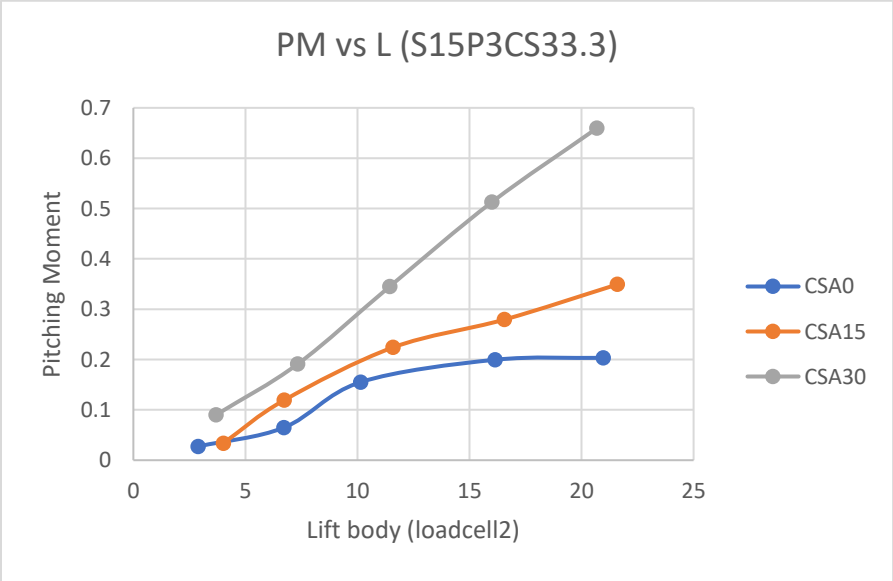

b) Propeller 15inch located at 30%C from wing leading edge with the elevon size of 33.3%C.

Figure 32: Effect of Control Surface's Deflection Angle on the Pitching Moment

Size of Control Surface

Pitching moment at CG (25%C) is plotted with lift force. For most cases, either change propeller size, or change propeller position, it is found that the control surface's size of 33.3%C generates the highest pitching moment and the control surface's size of 50%C has the poorest control power.

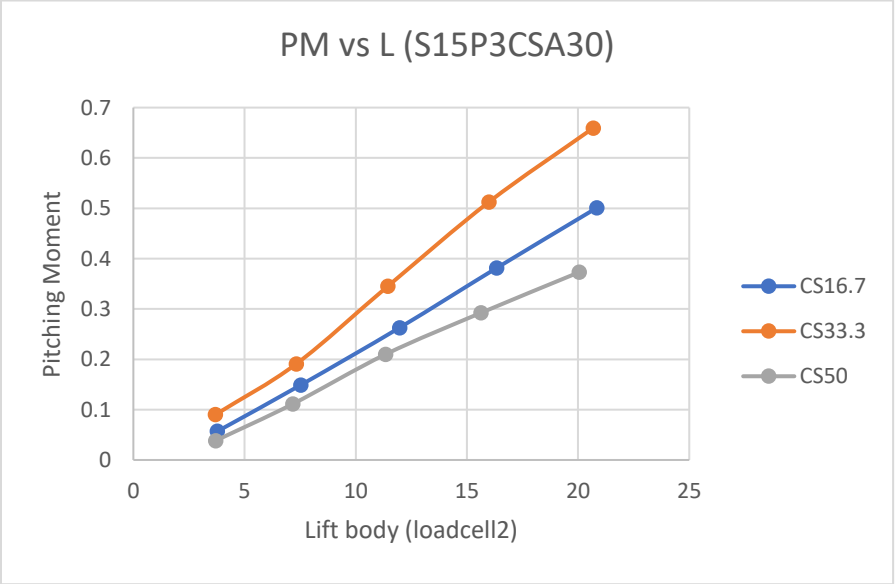

b. Propeller 15inch located at 30%C from wing leading edge with the elevon deflect of 30deg.

b. Propeller 15inch located at 10%C from wing leading edge with the elevon deflect of 30deg.

Figure 33: Effect of Control Surface's Size on the Pitching Moment

The trend of result is not same as estimate in the Table 2, this may result by 2 sources; a) highly reducing in the moment arm as mentioned in Table.2 and b) separation of flow on the control surface.

Position of Propeller

Example of the influence of propeller position on the elevon control power is illustrated in Fig.34. Install the propeller at 30%C ahead of wing leading edge gives the highest pitching moment when compared to install the propeller at 10 and 20%C.

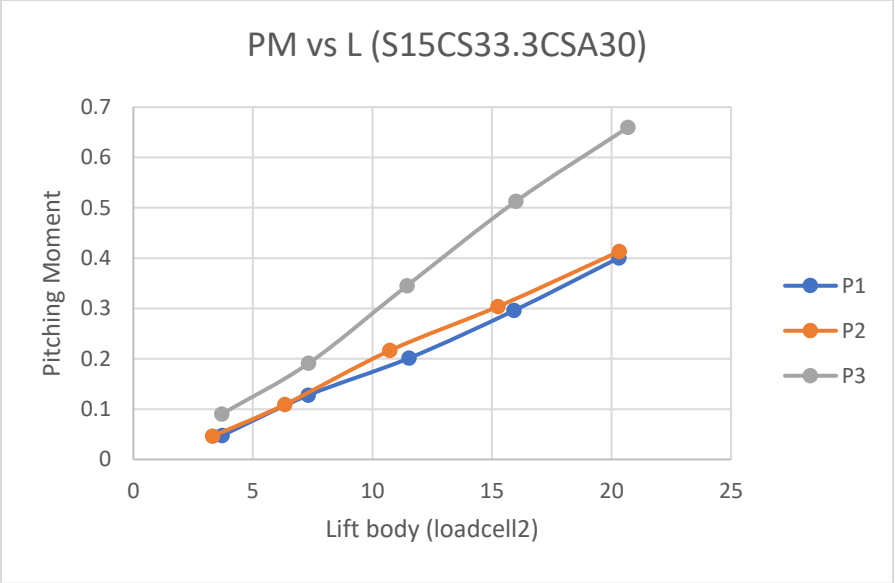

a) Propeller 15inch, Control Surface 33.3%C with the elevon deflect of 30deg.

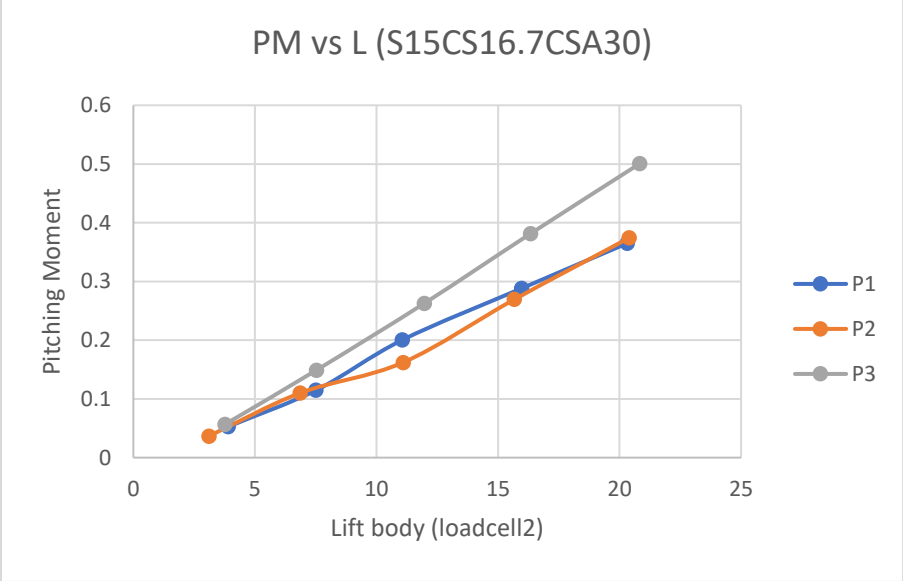

b) Propeller 15inch, Control Surface 16.7%C with the elevon deflect of 30deg.

Figure 34: Effect of Propeller Position on the Pitching Moment

Propeller Size

Fig.35a and b show the pitching moment for different propeller size from 13 to 17 inch at the propeller position 10%C and 30%C from wing leading edge respectively. For the close position, propeller at 10%C, the propeller size does not show clear significant influence to the pitching moment though the 15inch propeller configuration slightly best. For 30%C position, it is clear that the 15-inch propeller provides the most effective in term of elevon control power when compared to the other two wings with 13 and 17inch.

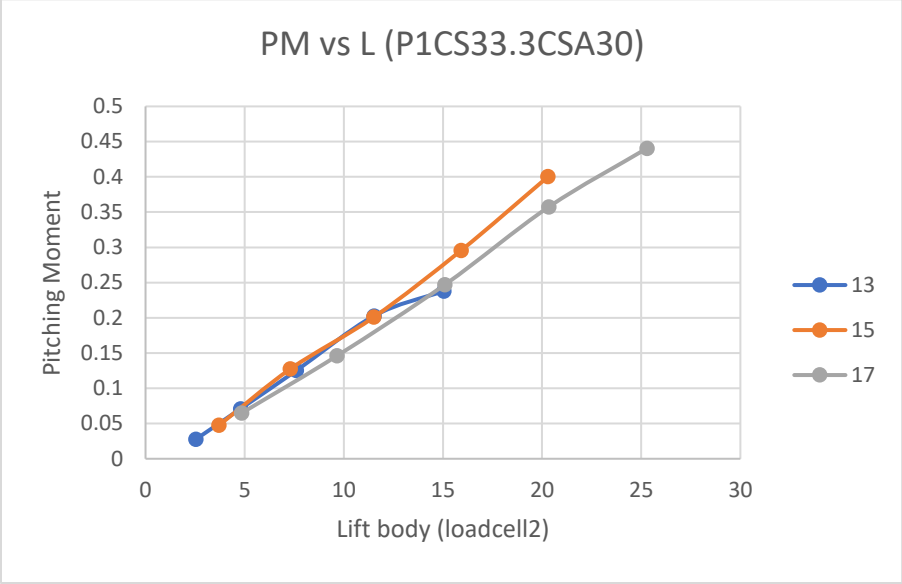

a) Propeller position 10%C, Control Surface 33.3%C with the elevon deflect of 30deg.

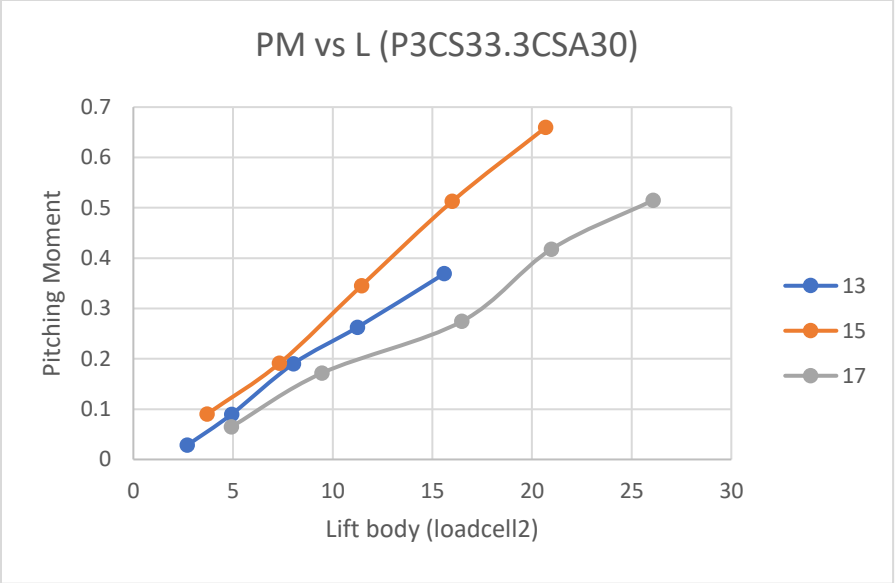

b) Propeller position 30%C, Control Surface 33.3%C with the elevon deflect of 30deg.

Figure 34: Effect of Propeller Size on the Pitching Moment

Test with Wind Condition

The test of pitching controllability of tail sitter during the vertical landing phase is conducted by place the wing trailing edge pace into the wind generator. The flow speed is set up at 5 m/s which is the maximum landing descend speed. The test is compared to the without wind conditions or stationary hover phase. The comparative test is performed at Propeller position 3 (30%C from leading edge), Control surface size of 33.3%C, and Propeller size of 13 and 15 inch with the throttle of 1200PWM and 1400PWM. The result shown in Fig 35-36 is plotted by lift force and pitching moment generated by the elevon deflection angle of 30 degree.

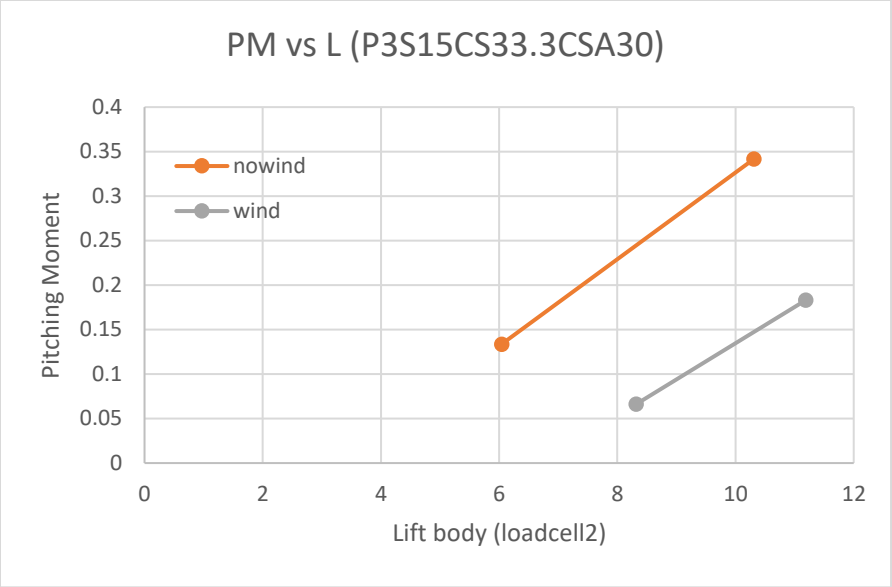

Figure 35: Effect of Wind (hover and landing phase)

Propeller Position 30%C, Prop Size 15 inch, Control Surface 33.3%C

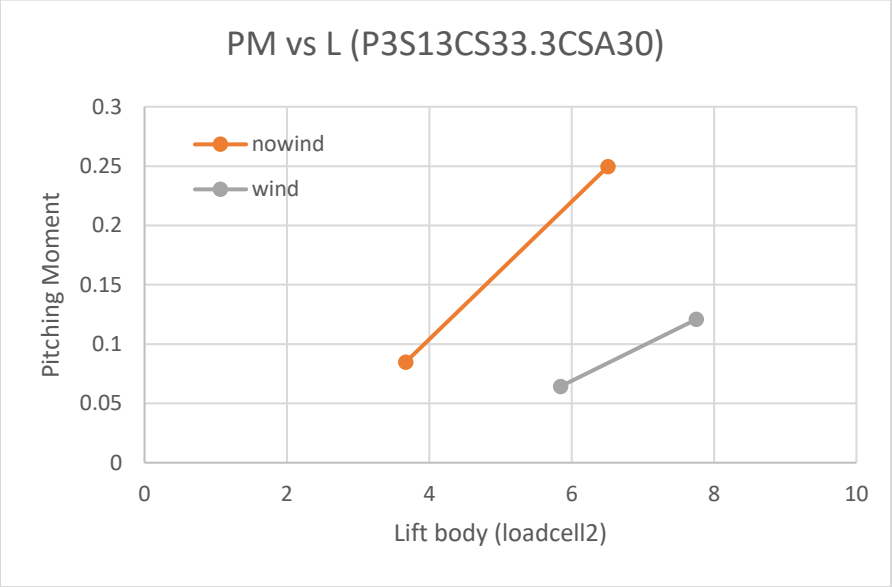

Figure 36: Effect of Wind (hover and landing phase)

Propeller Position 30%C, Prop Size 13 inch, Control Surface 33.3%C

As found in Fig.35-36, comparing with no wind condition, lift force is enhanced by the wind coming from the trailing edge. At the throttle of 1200PWM, lift increases from 6 Newtons to about 8.2 Newtons for the case of propeller size of 15 inch while the pitching moment at CG of wing is reduced from 0.135N.m to 0.065N.m. Similar result and trend for the case of propeller size of 15 inch at 1200 PWM, at the throttle of 1400PWM, lift increases from 10.5 Newtons to about 11.2 Newtons while the pitching moment at CG of wing is reduced from 0.35N.m to 0.18N.m. Left increases when the flow coming from trailing edge or when the tail-sitter UAV descents, which is opposite to the real. Therefore, pilot must highly reduce the throttle in order to make the aircraft vertically land. And this results in significantly decreasing of elevon control pitching moment as illustrated in the Fig.35-36. The similar result is found also in the case of propeller size of 13 inch. This investigation clearly shows the effect of flow from the trailing edge or the vertical landing phase of the tail-sitter configuration which introduce a high difficulty in attitude control of the aircraft during landing phase.

Conclusion

Tail-sitter UAV is one of interesting UAV and AAM platform due to its simple and less part and mechanism compared to other VTOL configuration such as a tiltrotor, a tilt-wing, and a combine propulsive type. For tail-sitter UAV with a twin tandem propeller type, it uses benefit of propwash induced flow from the propeller blowing pass into the control surface on the wing's trailing edge to control its attitude. However, the weak point of the tail-sitter configuration is the difficulty during the vertical hovering and in particular in landing phase. This research project is proposed to investigate and to find the optimal installation position of propeller, size of propeller, and size of control surface. Experimental test on the wing with propeller is set up. Control surface of wing model is designed to be adjustable with the size of 16.7%C, 33.3%C, and 50%C. Propeller diameter of 13 to 17inch is installed at 10%C, 20%C and 30%C from wing leading edge. Force and moment of the wing model is measured.

It is found that all three parameters: propeller size, propeller position, and control surface size, effect the elevon control power of the tail-sitter model. To compare the results, the lift and pitching moment are plotted. The configuration of wing with 33.3%C control surface, with the 15 inch diameter propeller installed at 30%C from leading edge provide the highest pitching moment during the vertical hovering phase.

The test with wind is then conducted by placing the wing model in front of a wind generator. The blowing speed is set at 5 m/s represents the case of tail-sitter UAV is landing to the ground with the decent speed of 5m/s. The result shows that, at an identical PWM signal command, the lift force of wing model is higher than the case of no wind conditions which may resulted from 2 reasons: reduction of propwash-force and increasing of thrust. (Since lift of model is the thrust minus propwash force.) Due to in flow coming from the trailing edge is opposite direction of propwash flow, this result in the lower wing speed passes the elevon or control surface.

Problems

The main difficulty of doing the research in this project is finding Man and Student. It is hard to find an engineer and (master) student who interested in Aerospace field, since there is no aerospace engineering industry except a part production. Bachelor student can not fucus on the project as well as their knowledge and experience is not enough for doing a good research output.

Getting a grant, it is the first time Kasetsart University get this grant, there are a document and the process both from outside (from Asian Office of Aerospace Research and Development) and inside (Kasetsart University). Therefore, this issue results in the delay of getting the budget about 1 year from starting date.

The renovate of wind tunnel building which is initially planned to use. And the movement of the Department of Aerospace Engineering, the test can not be conducted during the movement period for about 2 months, as well as some damage of the equipment from the movement to new building as well.

Outcome: Wind Generator

Wind generator is built during this project for the test with wind condition, and this equipment can be used for future investigation and or other project.

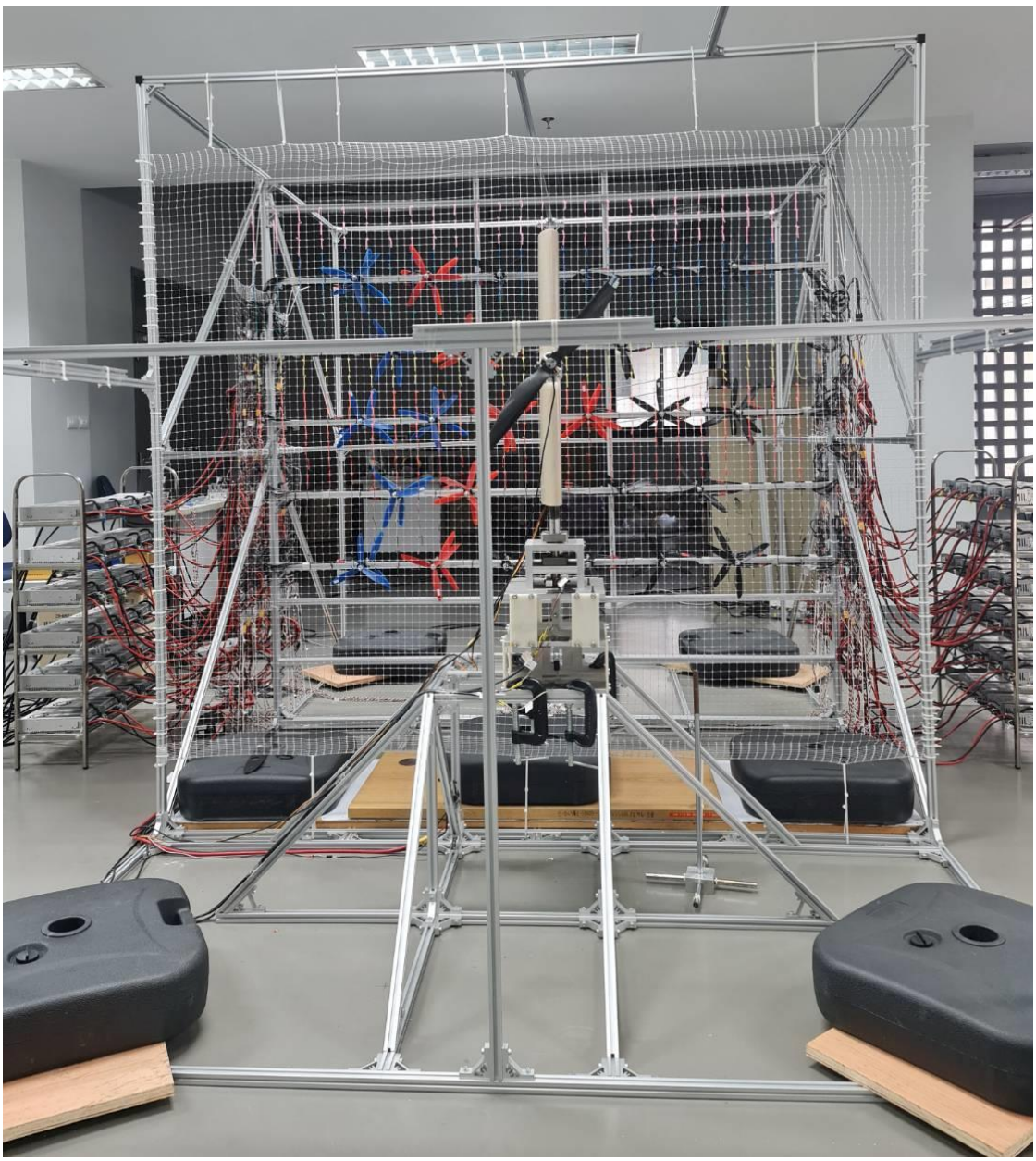

Outcome: Involved Student and Engineer

Year 1

4 Bachelor students, Aerospace Engineering department (10 months)

- Support the wing model and test set up.
- Conduct the test, Process the test result.
- Conceptual Design and Analysis of Tail-Sitter

1 Master student from mechanical engineering department (6 months)

- Write the measurement Labview Code

2 Engineers (10 months)

- Design the model and select all components of wing model.
- Prepare and select all equipment.

Year 2

3 Intern students (5 months)

- Design and select part and material for the wind generator.
- Set up the wind generator.
- Write the code for wind generator.

2 Bachelor students (2 months)

- Conduct the test.
- Process the test results.

1 Master student (2 months)

- Test with wind.
- Process the test results.

Outcome: Publications

1. Submitted for AIAA Conference (2024)

Aviation Technical Paper (Completed Research), Submission Received (4056178)

ผู้ส่ง Co-Located 2024 AIAA AVIATION Forum and 2024 ASCEND
ผู้รับ fengcpt@ku.ac.th
คัดลอก fengcpt@ku.ac.th
ตอบกลับ conferencepapers@aiaa.org
วันที่ 2023-12-13 01:59

Summary Headers Plain text

Tuesday, 12-Dec-2023

chinnapat thipyopas has successfully submitted:

Control ID: 4056178
Title: Aerodynamic Test of Elevon Control Power of Tail-Sitter VTOL in Hover Mode
Category: Applied Aerodynamics: Aero-Propulsive Interactions and Aerodynamics of Integrated Propeller Systems
Presentation Type: Aviation Technical Paper (Completed Research)

to the Co-Located 2024 AIAA AVIATION Forum and 2024 ASCEND.

Please retain a copy of this message. Notification of your submission status will be sent to you at this email address on or about 18 March.

You may continue to make changes to your abstract up to the deadline, 2000hrs/8pm Eastern Time 12 Dec. To do so, select "Edit/Return to Draft" from the dropdown box in the Take Action column. You must then re-submit before that deadline. Failure to re-submit at Step 5 will leave your submission ineligible for consideration.

AIAA policy discourages submitting the same abstract to multiple AIAA conferences for consideration. Overlapping submissions may result in your paper being withdrawn to avoid duplicate papers being published in the conference proceedings.

If interested in having this submission also considered for publication in one of AIAA's 8 peer-reviewed journals, please visit https://www.aiaa.org/publications/journals/Journal-Author for more information on Journal scopes, author resources and manuscript submission.

This is an automatically generated system email. Please do not respond to it. If you have questions, please contact Kim Grant, KimG@aiaa.org.

2. Related work had been done and published in SAWAE2022

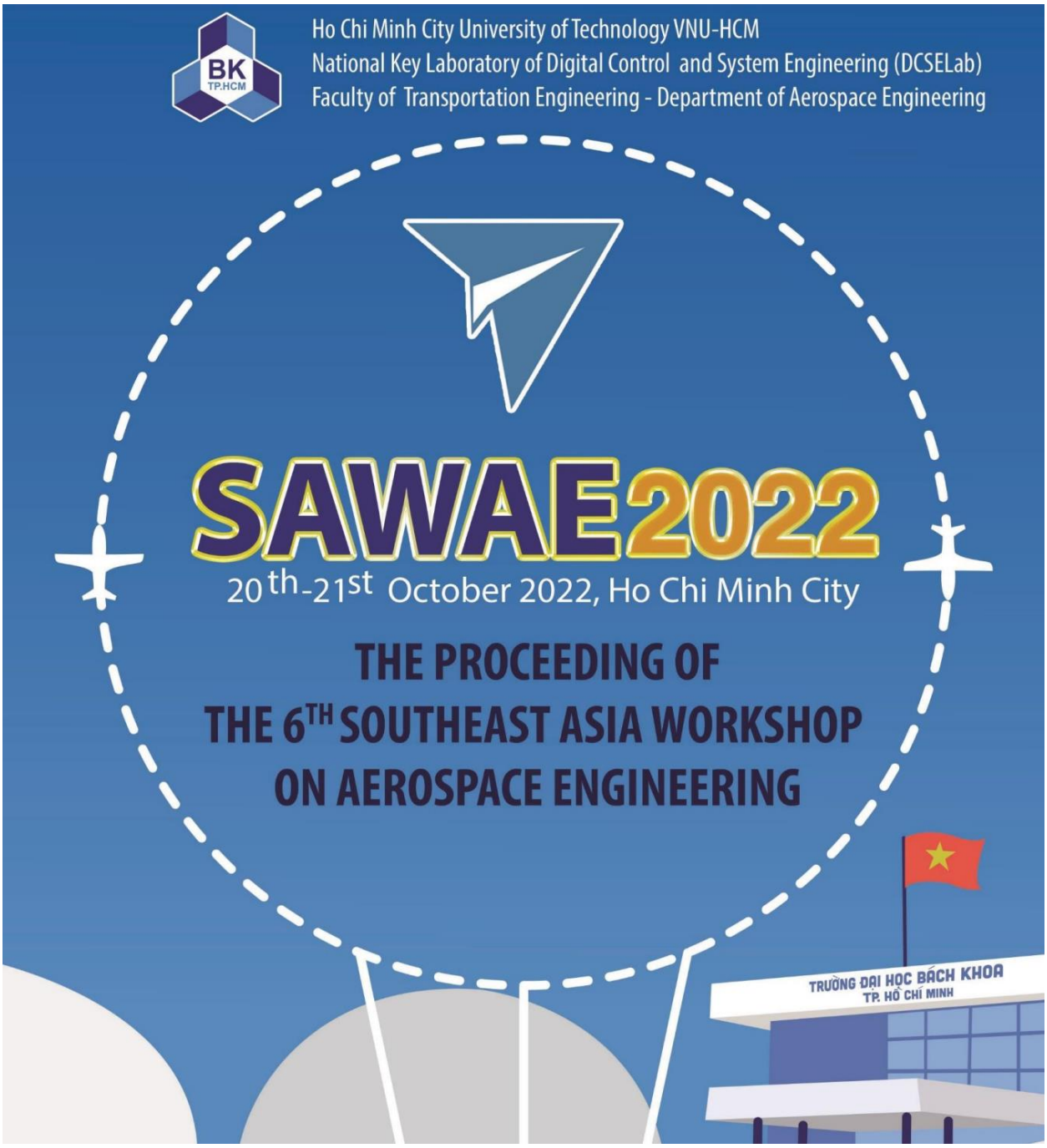

THE 6TH SOUTHEAST ASIA WORKSHOP ON AEROSPACE ENGINEERING (SAWAE2022)
OCTOBER 20TH – 21ST, 2022, HO CHI MINH CITY UNIVERSITY OF TECHNOLOGY, VNU-HCM, VIETNAM

SAWAE-2022-036
Analysis and Preliminary Design of Tail-Sitter Vertical Takeoff and Landing UAV 5*

Chinnapat Thipyopas [1], Narongdej Ongpalakon [1], and Narawara Sueyingkarn [1]
[1]*Department of Aerospace Engineering of Kasetsart University 50 Ngam Wong Wan Rd., Ladyaow, Chatuchak District, Bangkok 10900, Thailand.*

Email address: fengcpt@ku.th, narongdej.o@ku.th, and narawara.s@ku.th

ABSTRACT

In nowadays, it is accepted that unmanned aerial vehicles (UAVs) are worked instead of humans in case of safety and convenience for transportations and logistics in everyday life. In this thesis we focus on one of VTOL UAV called Tail-Sitter, aircraft that takes off and lands vertically also tilts to forward flight horizontally, which combines ability of fixed wing and rotary wing aircraft together. So it can operates missions in some limited runways. Therefore, Tail-Sitter contains both advantages and disadvantages of aircraft properties. The main weaknesses that we observe are short endurance in cruising performance, and low stability problems about hovering drag from perpendicular wind. Then we aim to improve it in a better way. First, we try to collect and study many informations from several researches to recognize various case of problems. We choose to design the better model based on analytics through calculations, trade studies and research results. We compare how many rotors in which airframe configurations either monoplane, biplane or canard wing perform better. As the result, we will receive at least one new model that improve aerodynamic and stability problems from the reference one.

Keywords: Tail-Sitter UAV, Vertical Take-Off and Landing (VTOL)

I. INTRODUCTION

5

From the past till present, unmanned aerial vehicles or UAVs have been one of the continuously evolving aviation industry using for several applications such as mapping, monitoring, searching, rescue, etc. The growth of the technology in aviation business has resulted in the UAVs development to become more accessible. Therefore, they have begun to be applied in various missions. Often, there are many problems occurred that they cannot perform some missions fluently that must be landed in the limited area. Thus, vertical take-off and landing UAV were created to perform this case in limit of using large amount of energy to drive the motor and slower flight performance. UAVs are divided into two main categories: Vertical take-off and landing aircraft and fixed-wing aircraft. Both of these types have different advantages and disadvantages. Therefore, various deficiencies were fixed by combining the two types of UAVs to form a hybrid unmanned aerial vehicle. The vertical take-off and landing of the vertical tail-mounted unmanned aerial vehicle called Tail-Sitter is a type of hybrid unmanned aerial vehicle that take advantage of each type of UAV to improve some characteristic performance. However, a tail-sitter also has significant problems with wind effects cause to lacking of stability while hovering, and low flight endurance due to wing limitations. So we have joint idea to analyze and design new model of Tail-sitter UAV by validation from flight test reference to be used in academic information and the development of aircraft technology in the future.

II. SETUP AND METHODOLOGY

Tail-sitter is one of hybrid UAV or Unmanned aerial vehicles that contain both advantage and disadvantage from variable of aerodynamic performance depend on several applications. Tail-sitter also has the main aircraft characteristic performance that must considered are thrust, drag, lift and weight of aircraft too.

2.1. Aerodynamics Drag

Total of drag is considered due to parasite drag, induce drag and wave drag.
The zero-lift drag is choose by component built up is one of calculate of drag in each component.

$$C_{D0} = \sum_{i=1}^{n} C_{f,i} FF_i Q_i \frac{S_{wet,i}}{S_{ref,i}} + C_{D,misc} + C_{D,L+P} \quad (1)$$

Skin friction drag is a type of aerodynamic drag, which is resistant force exerted on an object moving in a fluid. It is caused by the viscosity of fluids and is developed from laminar drag to turbulent drag as a fluid moves on the surface of an object.

$$C_f = \frac{1.328}{\sqrt{Re}}$$

Pressure drag is caused by the air particles being more compressed on the front-facing surfaces and more spaced out on the back surfaces. While FFw is form factor of wing relative to pressure drag. And FFf is form factor of fuselage

$$FF_w = \left(1 + \frac{0.6}{x_t}\left(\frac{t}{c}\right) + 100\left(\frac{t}{c}\right)^4\right)(1.34\, M^{0.18}(cos\ cos\ \varphi_m)^{0.28})$$

$$FF_F = 1 + \frac{60}{(\frac{l_F}{d_F})^3} + \frac{\frac{l_F}{d_F}}{400}$$

$$C_p = \frac{\Delta p_{stat}}{p_{dyn,\infty}} = \frac{p_{stat} - p_{stat,\infty}}{\frac{1}{2}\rho v_\infty^2}$$

$$C_p = 1 - \frac{v}{v_\infty}$$

Induced Drag is an inevitable consequence of lift and is produced by the passage of an airfoil through the air.

$$C_{Di} = KC_L^2$$

Interference Drag is drag that is generated by the mixing of airflow streamlines between airframe components such as the wing and the fuselage, the engine and the wing. Q is represented the interference factor.

Table 1 Interference factor chart

Interference factor with respect to ...	Property	Interference factor Q
nacelle	engine mounted directly on the wing or fuselage	1.5
	distance of engine to wing respectively fuselage is *smaller* than engine diameter d_N	1.3
	distance of engine to wing respectively fuselage is *greater* than engine diameter d_N	1.0
wing	high-wing, mid-wing or low-wing position *with* aerodynamically optimized wing-fuselage fairing	1..0
	low-wing position *without* aerodynamically optimized wing-fuselage fairing	1.10 ... 1.40
fuselage	-	1.0
horizontal or vertical tailplane	conventional empenage	1.04
	H-tail	1.08
	V-tail	1.03

Propeller can generate thrust by airspeed after propeller has more velocity also contain more drag. We can calculate propeller velocity by momentum theory and fixed control volume.

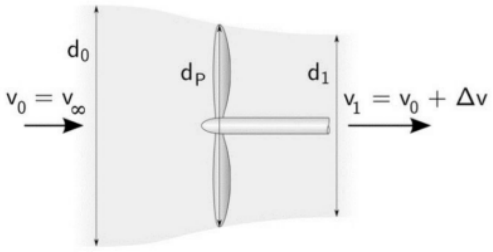

Figure 1 Aircraft velocity after propeller

Bernoulli's solution converts pressure difference to Kinetic energy per unit volume.

$$T = \frac{1}{2}\rho A_p(v_1^2 - v_0^2)$$

After that we can calculate drag by exit velocity.

$$D = \frac{1}{2}\rho v_1^2 S C_{D0}$$

2.2. Aircraft Power

When we know drag and flight velocity in the design. It is also important to calculate the power requirements for the engine in order to develop enough thrust to the engine or propeller to overcome possible drag.

2.3. Control Surface

Control surface we use to stabilize our tail-sitter are Elevons. Elevons are aircraft control surfaces that combine the functions of the elevator (used for pitch control) and the aileron (used for roll control). They are frequently used on tailless aircraft such as flying wings.

2.4. Reference Research

We have selected the research of Tail-sitter from Nolee, Teerawat and Chachavalvutikul, Norawit which studies and compares validation of calculation performance and test flight results. To use the results obtained as a guideline for choosing a more efficient aircraft design. In this research, a batt model aircraft flight with aerodynamic data was tested.
Starting from estimating the weight of 2 parts as follows:
1. Fixed weight is the total weight of the equipment when the machine size is changed. The weight in this section is fixed
2. Variable weight is the weight that depends on the structure, motor and battery when it is

changed.

Table 2 Batt model Characteristics

Empty weight - structure - battery -avionic -etc. motor , servo , navigation , connecting , no board computer	4 kg 2 kg 1.14 kg 0.1 kg 0.76 kg
Motor	Sunny-sky X3520
Propeller	APC 13*8
Airspeed	3 m/s
Circular flight cruise	800 m
Time of flight	53 minutes
Battery remain	40-50%

Figure 2 VETAL Batt model

2.5. Design Motivation

First we input 2 case problems of Tail-sitter UAV design for fixed them and improve more efficiency. After that, we continued to expand each case of problems by preliminary design. Evaluate difference case for choose the best one.

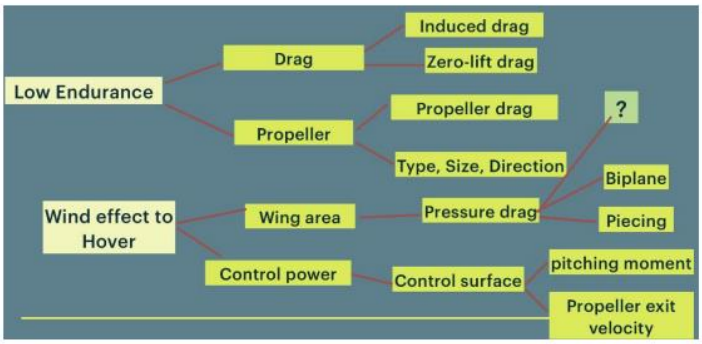

Figure 3 Preliminary problem diagram

III. RESULTS AND DISCUSSION

This section will well discuss the experimental results. Firstly, the concept of the tail-sitter's problems will be expanded to large variation that we have willing to analyze.

3.1 Analysis of new Tail-sitter models

3.1.1. Cause's diagram of Tail-sitter problems

Two mains of Tail-sitter problems are

1. Low endurance in horizontal flight
2. Large amount of drag in vertical flight

We have researched , studied and collected many researches to summarized this diagram .

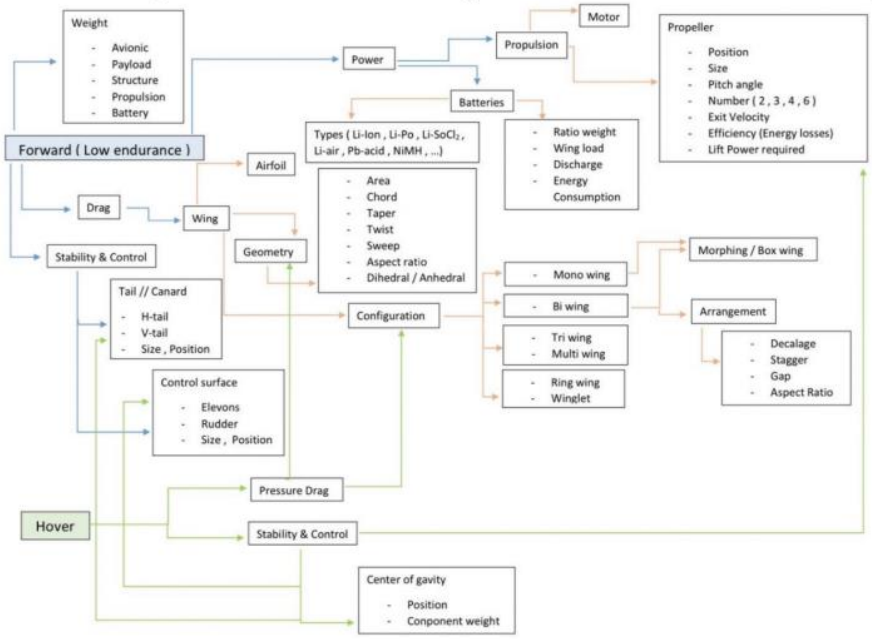

Figure 4 Cause's diagram of Tail-sitter problem

3.1.2. New Tail-sitter trends

If we look at diagram in fig.2 , It have many factors can cause problems in horizontal flight and vertical flight. Therefore, we look for starting point to design the new model. Then we began to consider configuration of wing and number of propellers by reason of these two things are important. There is a connection between horizontal flight problems and vertical flight problems.

Configuration of wing, we chose Canard, Mono-wing and Bi-wing to consider because the multi-wing is bad in structure and has a huge impact on weight. The mono-wing and bi-wing can generate enough lift while canard solves the stability problem.

Number of propellers we chose 2 , 4 , 6 to consider. Having an odd number of blades can cause stability and control problems because usually the blades rotate in opposite directions to balance the UAV, it's more complicated than necessary. Then we have nine types of tail-sitter but it must be considered to

1. Aspect Ratio
2. Propeller diameter
3. Position of propellers
4. Elevons
5. Space of two wings (Canard)
6. Gap of two wings (Biplane)

3.2. Batt Model Validation

The calculation will refer to the calculation method from the research named Design and Build Tail-sitter Vertical Takeoff and Landing Aircraft by Mr. Teerawat Nolee and Mr. Norawit Chatchawanwuthikul, 2017. To compare the author's calculations and the results of the actual flight test. All input values are based on the aforementioned research.

3.2.1. Calculate the approximate weight of Tailsitter

Table 3 The approximate weight of Tailsitter

List	Autopilot	ESC	Servo	Wire	Propeller	Payload	Structure	Motor	Battery	Total
Weight (g)	176	160	56	194	68	236	1500	650	1200	4240

3.2.2. Calculate the wing area of Tailsitter , chose airfoil and design the wings in the program

1) Calculation of wing area

Table 4 Calculate wing area

Weight	41.59	N
Maximum Lift Coefficient	0.8	
Minimum Airspeed	12	m/s
Air Density	1.225	kg/m3
Wing Area	0.589	m2

2) Fauvel Airfoil

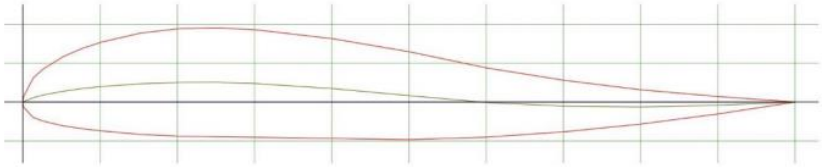

Figure 5 FAUVEL Airfoil

3) Designing bat-wing in XFLR5

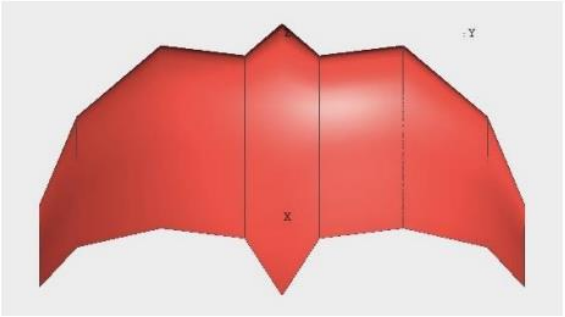

Figure 6 Batt model from XFLR5

3.2.3. Calculate the new weight of structure

Table 5 The new weight of structure

List	Wing	Fuselage	Elevon	Fin	Glue & Epoxy	Total
Weight (g)	705	465	88	284	58	1600

3.2.4. Calculate the thrust required and select the motor.

1) Find the Drag of the tailsitter. It is divided into 2 parts, namely the total Drag of the tailsitter and the drag of the wing area after propeller.

Table 6 Total drag of the BATT model

C_{D0} wing	0.009014
C_{D0} body	0.00287
C_{D0} motor block	0.0674
C_{D0} fins	0.0345
C_{D0} total	0.1138

Table 7 Drag of wing and avionics after propeller of the BATT model

C_{D0} wing after propeller	0.003235
C_{D0} motor block after propeller	0.0337
C_{D0} total after propeller	0.03694

2) Find the thrust required for both stages of flight. The thrust required for the motor is 22.15 newtons for vertical flight and 9.48 newtons for horizontal flight.

Table 8 Thrust required for horizontal flight

D1 (N)	D2 (N)	D3 (N)	∑D (N)	V^2 (m^2/s^2)	NewD3 (N)	ΔD3 (N)
17.80	2.98	2.98	17.80	546.34	4.07	1.09
		4.07	18.89	555.29	4.13	0.07
		4.13	18.96	555.84	4.14	0.004
		4.14	18.96	555.87	4.14	0.0002
		4.14	18.96	555.87	4.14	0.00

3) Choose a motor that drives more than 22.15 newtons, so choose T-MOTOR U7 490KV with a weight of 299 grams each.

3.2.5. Convert thrust to power

Table 9 Convert thrust to power by calculation

	Hover Phase		Cruise Phase	
	1 Motor	Total	1 Motor	Total
Thrust (N)	22.15	44.30	9.48	18.96
Power (W)	473.36	946.72	210.71	421.41

Based on the power required, given the vertical take-off and landing time is 3 minutes, a battery capacity of 2,132.26 mAh per hour is required. The horizontal flight, given the cruise time is 20 minutes at 20 meters per second. It will require a battery capacity of 9,491.30 mAh per hour. The total battery capacity is more than 11,623.56 mAh per hour, so chose the Lipo 6s battery, which weighs 1201 grams.

Recalculate the new weight in place of the estimated weight.

3.2.6. Replaced the estimated weight with the new weight and recalculated the thrust and power, found that the same motor and battery could be used.

Table 10 New weight of Batt model

List	Autopilot	ESC	Servo	Wire	Propeller	Payload	Structure	Motor	Battery	Total
Weight(g)	176	160	56	194	68	236	1600	600	1201	4291

Table 11 New power required of Batt model

Thrust (N)	22.42	44.84	9.50	19.00
Power (W)	481.37	962.74	211.10	422.20

3.2.7. Compare test results with calculations.

Cruise at a speed of 20 meters per second.

Table 12 Comparing test results with calculations

Hover Power (W)			Cruise Power (W)		
Test	Calculate	Error	Test	Calculate	Error
1005.66	962.74	-4.27 %	440.67	422.20	-4.19 %

3.3. Vetal Model Validation

The wing shape of the Vetal model is the same as the Batt model. The Vetal's weight and wing area estimates are the same as the Batt, but the Vetal cruises at 15m/s, uses a 13-inch diameter propeller, uses a Sunnysky X3520 kv520 motor, a maximum thrust of 4000g and uses a Battery model Li-ion 6s 4p 12000 mAh per hour, Test flight for 53 minutes.

3.3.1. Calculate the thrust required

1) Find the Drag of the tailsitter. It is divided into 2 parts, namely the total Drag of the tailsitter and the drag of the wing area after propeller.

Table 13 Total drag of the Vetal model

C_{D0} wing	0.009058
C_{D0} body	0.003032
C_{D0} motor block	0.0674
C_{D0} fins	0.0345
C_{D0} total	0.1145

Table 14 Drag of wing and avionics after propeller of the Vetal model

C_{D0} wing after propeller	0.002996
C_{D0} motor block after propeller	0.03387
C_{D0} total after propeller	0.03686

2) Find the thrust required for both stages of flight. The thrust required for the motor is 22.26 newtons for vertical flight and 9.48 newtons for horizontal flight.

Table 15 Thrust required for vertical flight

2T (N)	T (N)	V^2 (m^2/s^2)	D (N)	2D+W (N)	∑F (N)
41.59	20.80	396.51	1.3652	44.32	-2.73
44.32	22.16	422.54	1.4549	44.50	-0.18
44.50	22.25	424.25	1.4607	44.52	-0.01
44.52	22.26	424.36	1.4611	44.52	-0.0008

211

44.52	22.26	424.37	1.4611	44.52	0.00

Table 16 Thrust required for horizontal flight

D1 (N)	D2 (N)	D3 (N)	∑D (N)	V^2 (m^2/s^2)	NewD3 (N)	ΔD3 (N)
11.75	1.55	1.55	11.75	337.05	2.32	0.77
		2.32	12.53	344.40	2.37	0.05
		2.37	12.58	344.88	2.37	0.003
		2.37	12.58	344.91	2.38	0.0002
		2.38	12.58	344.92	2.38	0.00

3) Sunnysky X3520 kv520 motor can handle 2269.72g load.

3.3.2. Convert thrust to power

Table 17 Convert thrust to power by calculation

	Hover Phase		Cruise Phase	
	1 Motor	Total	1 Motor	Total
Thrust (N)	22.26	44.52	6.29	12.58
Power (W)	435.12	870.24	94.35	188.69

Based on the power required, given the vertical take-off and landing time is 3 minutes, a battery capacity of 2,940 mAh per hour is required. The horizontal flight, given the cruise time is 50 minutes at 15 meters per second. It will require a battery capacity of 10,624.52 mAh per hour. The total battery capacity is more than 13,564.52 mAh per hour, The Vetal model uses a

Li-ion 6s 4p 12000 mAh battery. Therefore, the calculated battery capacity has an error of 13.04% .

3.4. Analysis of the results of the validation

From the calculation, it can divide a calculation into two main parts: the calculation of the Tailsitter in vertical flight and the calculation of the Tailsitter while flying horizontally.

1) Calculation of the Tailsitter while flying vertically

- The drag varies to the area of the wing perpendicular to the wind.
- If using a smaller propeller, the drag of the wing after the propeller is more valuable. Because the speed behind the propeller must be greater to achieve the same thrust. And if there is no propeller on the wing, there is no drag caused by the propeller.

2) Calculation of the Tailsitter while flying horizontally

-Longer wings are aerodynamically better, but the tail-sitter has to transition, wings with a lower aspect ratio are preferred to avoid wing twisting.

- If using a smaller propeller, the drag of the wing after the propeller is more valuable. Because the speed behind the propeller must be greater to achieve the same thrust. And if there is no propeller on the wing, there is no drag caused by the propeller.

3.5. Design Variation Tail-Sitter Model from XFLR5

After calculating the validation results, compare them with the test flight. We have used XFLR5 as a tool to determine the performance characteristics of a wide range of Tail-Sitter aircraft. Configuration of the wings are Monoplane, Biplane and Canard as selected above. Which the various forms have designed the wings as a rectangular wing as a base structure by adjusting the Aspect Ratio to be 4 different values of each configurations to 2, 2.5, 3 and 3.5 through 14% FAUVEL AIRFOIL set the total wing area to be the same size at 0.589 square meters and consider all models to compare with the Batt model as well. Airspeed 20 meters per second. Air density 1.225 kg/m3

In the Canard model, we have separately determined the separation of the main wing and the Canard wing by 100% Chord and 150% Chord, while in the Biplane model we have set the distance between the upper wings and the lower wing (Gap) 100% Chord and 150% Chord as well. We also created another variant of the Biplane, which the publisher considers another interesting design by adding Biplane to look like Morphing wing, defined as Box wing, adding that the upper wings of the Biplane can be folded down to form a box. which contributes to the stabilization of the aircraft in different postures.

When focusing the feature of Morphing wing that can adjust the form of the wings while in flight. So we have tried to increase the case of reducing the area of impact when flying. and increase aerodynamic properties while flying. By giving the wings a longer appearance at Aspect Ratio 5 for Monoplane and Canard to consider too.

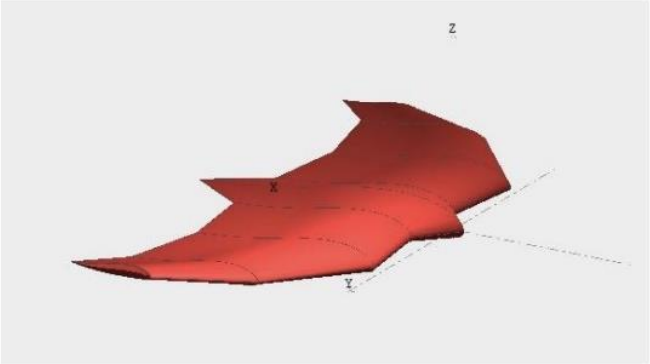

Figure 7 XFLR5 Analysis Model

3.6. Efficiency analysis 's based on the appropriate lift coefficient to drag coefficient ratio.

3.6.1. Appropriate AoA

This is the angle that creates the best lift that can support the aircraft in flight conditions. A minimum lift force equal to the aircraft's weight of 42.0947 N is required, analyzed from the Fz - Alpha relationship curve of each configuration.

3.6.2. Lift Coefficient and Drag Coefficient

From the reference area in each configuration analysis via XFLR5, when the lifting force is equal to the aircraft weight is determined. We can calculate the lift coefficient of all forms. The resistance coefficient was then analyzed through the CL – CD relationship curve.

3.6.3 Analyze the appropriate Lift coefficient to Drag coefficient ratio.

Analyzed through the CL/CD – Alpha relationship graph at the appropriate angle of impact. which will have similar results as taking the lift coefficient and the coefficient of resistance from step 3.6.2. Then divide them together.

3.7. Stability and Moment Performance Analysis

3.7.1. Determine Flaps Angle

Designed to open the control surface angle (Elevons) with reference to 27% Chord of FAUVEL 14% AIRFOIL design effect of opening angle increased every 5 degrees.

3.7.2. Flaps position, maximum open angle and maximum moment coefficient

Configure the Flaps Opening Angles for each aircraft pattern to see the trend for the maximum Flaps angle position. By analyzing the angle opening pattern through the Cm–Alpha relationship graph, it is found that as the Flaps angle increases gradually. The moment coefficient continues to increase in a straight line. At some point the moment coefficient cannot be read in the graph. We therefore estimate that point, consider the opening position, the maximum angle flaps, and analyze the maximum moment coefficient at that point.

3.7.3. Moment analysis of the control surface effect

Now that we know the maximum moment coefficients obtained by setting different flaps angles. The lifting force equals the weight of the machine at a speed of 20 meters per second. We can calculate the moment of an aircraft equipped with Elevons.

3.7.4. Analysis of the pitching moment caused by the force of the propeller during vertical flight.

From the xflr5 program, we can find the moment caused by the control surface, but if the wing has 4 or 6 propellers, the control surface is not necessary. We use mathematical methods to calculate the case dimensions according to the xflr5 and analysis 5.4. then we focused on larger propellers at a given wing span. But if the wings are too short, the case will be cut out of consideration as follows:

Table 18 Moment analysis of propeller forces during vertical flight

	Aspect Ratio	Main span (m)	Total Thrust of 4 propellers (N)	Moment arm of 4 propellers (m)	Total Thrust of 6 propellers (N)	Moment arm of 6 propellers (m)
Monoplane	2	1.0854	41.5944	1.5031	43.0637	1.9697
	2.5	1.2135	41.5944	1.5031	42.8953	1.9582
	3	1.3293	41.5944	1.5031	42.7729	1.9499
	3.5	1.4358	41.5944	1.5031	42.6792	1.9437
	5	1.7161	41.5944	1.5031	42.5644	1.9360
Canard	2	0.9708	41.5944	1.5031	42.8953	1.9582
(space = 1C)	2.5	1.0854	41.5944	1.5031	42.7473	1.9482
	3	1.1889	41.5944	1.5031	42.6397	1.9411
	3.5	1.2842	41.5944	1.5031	42.5570	1.9356
	5	1.5349	41.5944	1.5031	42.5058	1.9322
Canard	2	0.9708	41.5944	1.5031	42.8953	1.9582
(space = 1.5C)	2.5	1.0854	41.5944	1.5031	42.7473	1.9482
	3	1.1889	41.5944	1.5031	42.6397	1.9411
	3.5	1.2842	41.5944	1.5031	42.5570	1.9356
	5	1.5349	41.5944	1.5031	42.5058	1.9322
Biplane	2.5	0.8581	44.4053	1.6928	43.4271	1.9949
(gap = 1C)	3	0.9399	44.1356	1.6725	43.2547	1.9829
	3.5	1.0153	43.9293	1.6574	43.1224	1.9737
Biplane	2.5	0.8581	44.4053	1.6928	43.4271	1.9949
(gap = 1.5C)	3	0.9399	44.1356	1.6725	43.2547	1.9829
	3.5	1.0153	43.9293	1.6574	43.1224	1.9737
Boxplane (gap = 1C)	3.5	0.8494	43.5183	1.6279	42.8575	1.9557
Boxplane	3	0.8140	43.9221	2.0888	43.1178	2.6916
(gap = 1.5C)	3.5	0.8954	43.6310	1.6359	42.9303	1.9606

The table shows the moment arm of each case. The moment of each case was fixed to the moment of the Batt model equal to 37.7146 N*m using the MN3508 KV380 for the 4-blade motor and the MN3110 KV470 for the 6-blade case. The two types of the motor will support the thrust of all cases from 50 % to 60% throttles and the maximum throttle is 85%.

The number of propellers is divided into 2 sides by the wing. One side has more thrust than the other. where the greater side is the force generated by the maximum throttle and the lesser side is the thrust throttle minus the difference between the maximum throttle and the thrust throttle. Bring both sides of the force to find the moment arm. If any case has a larger moment arm, then It is more structurally complex and has less strength than other cases. The calculation results are subject to further trade studies.

Table 19 Final trade study chart

Configurations	Rotor	AR	S	Drag / Hover	T,total / H	Power / Hover	T,total / F	Power / Forward	M (Nm)	M,arm (m)	Pitching Stability	CL/CD	Aerodynamic	Summary
Monoplane	2	2	0.589	1.672325976	46.3368	4.488268504	22.7981	8.347916467	56.621256		8.782643135	13.55513267	7.118959109	30.41011319
		2.5	0.589	1.672325976	45.7573	4.550799796	22.2179	8.600236577	48.135369		7.466379156	15.13785444	7.950181631	30.23992314
		3	0.589	1.672325976	45.342	4.59561299	21.8283	8.769667661	64.469494		10	16.35125869	8.587443948	33.62505057
		3.5	0.589	1.672325976	45.0277	4.629527719	21.5487	8.891261426	38.535236		5.977282226	17.39454115	9.135360765	30.30575811
*Morphing		5	0.287	4.235993209	44.9451	4.638440721	21.295	9.001591678	29.212902		4.531275237	19.04089132	10	32.40730085
	4	2	0.589	1.672325976	41.5944	5	20.4646	9.362719943		1.5031	10	13.55513267	7.118959109	33.15400503
		2.5	0.589	1.672325976	41.5944	5	20.1964	9.479356022		1.5031	10	15.13785444	7.950181631	34.10186363
		3	0.589	1.672325976	41.5944	5	20.0241	9.554286658		1.5031	10	16.35125869	8.587443948	34.81405658
		3.5	0.589	1.672325976	41.5944	5	19.9056	9.605820497		1.5031	10	17.39454115	9.135360765	35.41350724
		5	0.287	4.235993209	41.5944	5	19.7035	9.693710697		1.5031	10	19.04089132	10	38.92970391
	6	2	0.589	1.672325976	43.0637	4.841454308	22.7981	8.347916467		1.9697	8.266458612	13.55513267	7.118959109	30.24711447
		2.5	0.589	1.672325976	42.8953	4.859625611	22.2179	8.600236577		1.9582	8.309184128	15.13785444	7.950181631	31.39155392
		3	0.589	1.672325976	42.7729	4.872833255	21.8283	8.769667661		1.9499	8.340020805	16.35125869	8.587443948	32.24229165
		3.5	0.589	1.672325976	42.6792	4.88294401	21.5487	8.891261426		1.9437	8.363055431	17.39454115	9.135360765	32.94494761
		5	0.287	4.235993209	42.5644	4.895331572	21.295	9.001591678		1.936	8.391662951	19.04089132	10	36.52457941
Canard 1C	2	2	0.589	1.672325976	45.7573	4.550799796	22.6177	8.426369669	39.651069		6.150361412	10.82831892	5.686876072	26.48673293
		2.5	0.589	1.672325976	45.2561	4.604882081	22.0814	8.65959834	34.67232		5.378097155	11.23115463	5.898439544	26.2133431
		3	0.589	1.672325976	44.8962	4.643717304	22.7224	8.38083724	30.661448		4.755962199	12.91289463	6.781665002	26.23450772
		3.5	0.589	1.672325976	44.6223	4.673272647	22.9946	8.262461621	26.063535		4.042770172	13.94982418	7.326245368	25.97707578
		5	0.3751	3.48811545	44.4538	4.69145474	21.1798	9.051690396	19.764313		3.065684561	15.95747605	8.380635012	28.67758016
	4	2	0.589	1.672325976	41.5944	5	20.5599	9.321275429		1.5031	10	10.82831892	5.686876072	31.68047748
		2.5	0.589	1.672325976	41.5944	5	20.2948	9.436563367		1.5031	10	11.23115463	5.898439544	32.00732889
		3	0.589	1.672325976	41.5944	5	20.1249	9.510450279		1.5031	10	12.91289463	6.781665002	32.56944126
		3.5	0.589	1.672325976	41.5944	5	20.0086	9.561027371		1.5031	10	13.94982418	7.326245368	33.55959872
		5	0.3751	3.48811545	41.5944	5	19.8175	9.64413384		1.5031	10	15.95747605	8.380635012	36.5128843
	6	2	0.589	1.672325976	42.8953	4.859625611	22.6177	8.426369669		1.9582	8.309184128	10.82831892	5.686876072	28.95438146
		2.5	0.589	1.672325976	42.7473	4.875595639	22.0814	8.65959834		1.9482	8.346336751	11.23115463	5.898439544	29.45229625
		3	0.589	1.672325976	42.6397	4.887206281	22.7224	8.38083724		1.9411	8.372715113	12.91289463	6.781665002	30.09474961
		3.5	0.589	1.672325976	42.557	4.896130074	22.9946	8.262461621		1.9356	8.393149056	13.94982418	7.326245368	30.55031209
		5	0.3751	3.48811545	42.5058	4.90165484	21.1798	9.051690396		1.9322	8.405780948	15.95747605	8.380635012	34.22787665
Canard 1.5C	2	2	0.589	1.672325976	45.7573	4.550799796	22.6177	8.426369669	39.964074		6.198912334	10.84759783	5.697001074	26.54540885
		2.5	0.589	1.672325976	45.2561	4.604882081	22.0814	8.65959834	34.376704		5.332243437	11.28675441	5.92763974	26.19668957
		3	0.589	1.672325976	44.8962	4.643717304	22.7224	8.38083724	30.401334		4.715615444	12.94032024	6.796068538	26.2085645
		3.5	0.589	1.672325976	44.6223	4.673272647	22.9946	8.262461621	25.326846		3.92850084	13.96050143	7.331852904	25.86841399
		5	0.3751	3.48811545	44.4538	4.69145474	21.1798	9.051690396	19.619066		3.043154885	15.89489771	8.347769777	28.62218525
	4	2	0.589	1.672325976	41.5944	5	20.5599	9.321275429		1.5031	10	10.84759783	5.697001074	31.69060248
		2.5	0.589	1.672325976	41.5944	5	20.2948	9.436563367		1.5031	10	11.28675441	5.92763974	32.03652908
		3	0.589	1.672325976	41.5944	5	20.1249	9.510450279		1.5031	10	12.94032024	6.796068538	32.97884479
		3.5	0.589	1.672325976	41.5944	5	20.0086	9.561027371		1.5031	10	13.96050143	7.331852904	33.56520625
		5	0.3751	3.48811545	41.5944	5	19.8175	9.64413384		1.5031	10	15.89489771	8.347769777	36.48001907
	6	2	0.589	1.672325976	42.8953	4.859625611	22.6177	8.426369669		1.9582	8.309184128	10.84759783	5.697001074	28.96450646
		2.5	0.589	1.672325976	42.7473	4.875595639	22.0814	8.65959834		1.9482	8.346336751	11.28675441	5.92763974	29.48149645
		3	0.589	1.672325976	42.6397	4.887206281	22.7224	8.38083724		1.9411	8.372715113	12.94032024	6.796068538	30.10915315
		3.5	0.589	1.672325976	42.557	4.896130074	22.9946	8.262461621		1.9356	8.393149056	13.96050143	7.331852904	30.55591963
		5	0.3751	3.48811545	42.5058	4.90165484	21.1798	9.051690396		1.9322	8.405780948	15.89489771	8.347769777	34.19501141
Biplane 1C	4	2.5	0.295	4.168081494	44.4042	4.696806857	21.7018	8.824680577		1.6928	9.295214742	12.31363483	6.466942446	33.45172612
		3	0.295	4.168081494	44.1356	4.7257903	21.3914	8.959668791		1.6725	9.370634566	13.08858027	6.873932553	34.09810771
		3.5	0.295	4.168081494	43.9293	4.748051225	21.1693	9.056256686		1.6574	9.426735027	13.5655782	7.124444951	34.52356938
	6	2.5	0.295	4.168081494	43.4264	4.802316949	21.7018	8.824680577		1.9949	8.172834002	12.31363483	6.466942446	32.43485547
		3	0.295	4.168081494	43.2547	4.82084434	21.3914	8.959668791		1.9829	8.217417149	13.08858027	6.873932553	33.03994433
		3.5	0.295	4.168081494	43.1224	4.83512025	21.1693	9.056256686		1.9737	8.251597562	13.5655782	7.124444951	33.43550094
Biplane 1.5C	4	2.5	0.295	4.168081494	44.4053	4.696688161	21.7023	8.824463134		1.6928	9.295214742	12.92359816	6.787286344	33.77173388
		3	0.295	4.168081494	44.1356	4.7257903	21.3914	8.959668791		1.6725	9.370634566	13.67349342	7.181120461	34.40529561
		3.5	0.295	4.168081494	43.9293	4.748051225	21.1693	9.056256686		1.6574	9.426735027	14.1399736	7.426109085	34.82523352
	6	2.5	0.295	4.168081494	43.4271	4.802241415	21.7023	8.824463134		1.9949	8.172834002	12.92359816	6.787286344	32.75490639
		3	0.295	4.168081494	43.2547	4.82084434	21.3914	8.959668791		1.9829	8.217417149	13.67349342	7.181120461	33.34713223
		3.5	0.295	4.168081494	43.1224	4.83512025	21.1693	9.056256686		1.9737	8.251597562	14.1399736	7.426109085	33.73716508
Box 1C	4	3.5	0.229	4.728353141	43.5183	4.792400425	21.0824	9.094048167		1.6279	9.536335265	14.68266709	7.711123836	35.86226083
	6	3.5	0.229	4.728353141	42.9303	4.855848915	21.0824	9.094048167		1.9557	8.318472284	14.68266709	7.711123836	34.70784634
Box 1.5C	4	3	0.197	5	43.9484	4.745990228	21.3916	8.959581814		2.0888	7.823970872	15.49676401	8.138675731	34.66821865
		3.5	0.2061	4.922750424	43.1347	4.833793011	21.0522	9.107181686		2.6916	5.584410759	15.39981339	8.087758674	32.53589455
	6	3	0.197	5	43.5183	4.792400425	21.3916	8.959581814		1.6359	9.506613166	15.49676401	8.138675731	36.39727114
		3.5	0.2061	4.922750424	42.8575	4.863704442	21.0522	9.107181686		1.9606	8.300267498	15.39981339	8.087758674	35.28166272
Batt	2	2.82	0.589	1.672325976	44.3048	4.707532674	18.9992	10	37.714546		5.849983327	16.12528773	8.468767276	30.69860925

IV. CONCLUSIONS

Tail-sitter design using calculate methods compared to the actual experiment, the results are good, can be adapted to a variety of formats. The calculation is divided into 2 cases: vertical flight and horizontal flight. In the analysis section, we want to solve the problems. Wind resistance while vertical flight and short flight time while flying horizontally. If want Tail-sitter performance better than the batt model must be analyzed by math model, XFLR5 and moment calculations. By using a larger propeller, the power consumption is lower, and the use of the control surface, generates more moment than the motor's unequal force according to the dimensions analyzed. According to trade studies, the best Tailsitter of each type is shown from the final table.

ACKNOWLEDGMENTS

Opportunity from faculty of Aerospace Engineering. We are extremely grateful to

Asst.Prof. Chinnapat thipyopas for his suggestion and assistance. We would like to thank Mr. Teerawat Nolee and Mr. Norawit Chatchawanwuthikul for their research, it was very helpful.

REFERENCES

[1] Ducard, G.J.J., and Allenspach, M. Review of designs and flight control techniques of hybrid and convertible VTOL UAVs. ETH Zürich, Zürich, Switzerland, 2021..
[2] David, L. (2014, Oct.). Guide & tutorial Pusher vs Tractor propeller configuration [Online]. Available: https://www.supermotoxl.com/resources/guides-tutorial/r-c-models-fpv-uav-diy-how-to-tips/pusher-vs-tractor-propeller-configuration.html.
[3] EPI Inc. (2020, Jan.). Propeller Performance Factors [Online]. Available: http://www.epi-eng.com/propeller_technology/selecting_a_propeller.htm.
[4] Heintz, C. Airfoils-Part 1. EAA Light Plane World, Oshkosh, May. 1987.
[5] HG Robotics Co.,Ltd. (2021). VETAL The new generation of VTOL drone for your survey business [Online]. Khlong Toei, Bangkok, Thailand. Available: https://www.hiveground.com/vetal/.
[6] Reddinger, J.P. Performance and Control Scalability of a Quadrotor Biplane Tailsitter. U.S. Army Research Laboratory, Aberdeen Proving Ground, MD, 2019.
[7] Vestlund, O. Aerodynamics and Structure of a Large UAV. Bachelor Thesis, Department of Science in Engineering-Aeronautics, Mälardalen University, Västerås, Sweden, 2018.
[8] Wang, H., Zhao, X., Bai, H., Lu, C., Zhang, B., and Li, C. Design of a Symmetrical Quad-rotor Biplane Tail-Sitter Aircraft without Control Surfaces and Experimental Verification. Department of Instrument Science and Engineering, Shanghai Jiao Tong University, Shanghai, China, 2018.

References

[1] Akshat Misra et al., A Review on Vertical Take-Off and Landing (VTOL) Tilt-Rotor and Tilt Wing Unmanned Aerial Vehicles (UAVs), Hindawi Journal of Engineering Volume 2022, Article ID 1803638

[2] Sarvesh Sonkar et al., Design & Implementation of an Electric Fixed-wing Hybrid VTOL UAV for Asset Monitoring, https://doi.org/10.1590/jatm.v15.1297

[3] Aurélien CABARBAYE, Design, model and control of a new type of VTOL aircraft, Doctoral Thesis, Institut Supérieur de l'Aéronautique et de l'Espace

[4] Win Ko Ko Oo et al., Design Of Vertical Take-Off And Landing (VTOL) Aircraft System, INTERNATIONAL JOURNAL OF SCIENTIFIC & TECHNOLOGY RESEARCH VOLUME 6, ISSUE 04, APRIL 2017

[5] Gesang Nugroho, Yoshua Dwiyanson Hutagaol and Galih Zuliardiansyah, Aerodynamic Performance Analysis of VTOL Arm Configurations of a VTOL Plane UAV Using a Computational Fluid Dynamics Simulation, Drones 2022, 6, 392. https://doi.org/10.3390/drones6120392

[6] Jean-Marc Moschetta , A Fixed-Wing Micro Air Vehicle with Hovering Capability, EOARD SPC 07-4010, Final Report for 06 July 2007 to 06 July 2010

[7] B. Bataillé, J.-M. Moschetta, D. Poinsot, C. Bérard and A. Piquereau, Development of a VTOL mini UAV for multi-tasking missions, The Aeronautical Journal , Volume 113 , Issue 1140: The International Powered Lift Conference 2008: A Special issue , February 2009 , pp. 87 – 98, DOI: https://doi.org/10.1017/S0001924000002815

[8] S. Shkarayev, J.-M. Moschetta, B. Bataillé, "Aerodynamic Design of Micro Air Vehicles for Vertical Flight", Journal of Aircraft, vol. 45, n°5, Sept.-Oct. 2008, pp. 1715-1724.

[9] Hao Wang et al., The Hovering Stability of the Egretta Tail-Sitter VTOL UAV, Hindawi International Journal of Aerospace Engineering Volume 2022, Article ID 9534180, 12 pages https://doi.org/10.1155/2022/9534180

[10] Verling, Sebastian et al., Full Attitude Control of a VTOL tailsitter UAV, IEEE International Conference on Robotics and Automation (ICRA 2016), Stockholm, Sweden, May 16-21, 2016

[11] Luiz F. T. Fernandez, Murat Bronz, Nathalie Bartoli, and Thierry Lefebvre, Development of a Mission-Tailored Tail-Sitter MAV, https://doi.org/10.1142/S2301385024430027

[12] Incremental control and guidance of hybrid aircraft applied to the Cyclone tailsitter UAV, E. Smeur, M. Bronz, G. D. Croon, Journal of Guidance Control and Dynamics, Feb 2018

[13] Helmi Abrougui et al., Roll Control of a Tail-Sitter VTOL UAV, International Journal of Control, Energy and Electrical Engineering (CEEE), Vol 7, pp.22-27

[14] O. Garcia, A. Sanchez, J. Escareño, R. Lozano, Tail-sitter UAV having one tilting rotor: Modeling, Control and Real-Time Experiments, Proceedings of the 17th World Congress The International Federation of Automatic Control Seoul, Korea, July 6-11, 2008

[15] Tri Kuntoro Priyambodo 1, Abdul Majid 2 , Zaied Saad Salem Shouran, Validation of Quad Tail-sitter VTOL UAV Model in Fixed Wing Mode, Journal of Robotics and Control (JRC) Volume 4, Issue 2, March 2023

[16] Ximin Lyu et al., Design and implementation of a quadrotor tail-sitter VTOL UAV, 2017 IEEE International Conference on Robotics and Automation (ICRA)

[17] K. Chinwicharnam, D. Gomez Ariza, J.-M. Moschetta and C. Thipyopas, « Aerodynamic Characteristics of a Low Aspect Ratio Wing and Propeller Interaction for a Tilt-Body MAV", International Journal for Micro Air Vehicles, vol. 5, n°4, Déc. 2013, p. 245-260.

[18] K. Chinwicharnam, D. Gomez Ariza, J.-M. Moschetta, C. Thipyopas, "A computation study on the aerodynamic influence of interaction wing-propeller for a tilt-body MAV". (2015) Aircraft

Engineering and Aerospace Technology: An International Journal, vol.87 (n°6). pp.521-529. ISSN 0002-2667

Funding Summary

Currency: United States dollar

Year 1

No.	Description	Planed	Used	Diff.
1	Wind Tunnel Models and Components (Model Fabrication, Part & Material)	5,000	(4,000)	-1,000
2	Force Measurement Equipment (Loadcell, Part & Material)	2,000	(1,000)	-1,000
3	Wind Tunnel Cost	-	-	
4	Engineering and Technician Support (Technician Support)	2,000	(1,000)	-1,000
5	Students / Research Assistants (Research Assistants 500*8)	5,000	(4,000)	-1,000
6	Researcher (Principal Researcher)	4,000	(4,000)	-
7	Report and Office Tools (Student and Office Material)	1,250	(1,250)	-
8	Transportations (Transportation in 1st year)	1,000	(1,000)	-
9	Conference and Related Expense	-	-	-
10	University Fees (University Free)	2,250	(2,250)	-
	Total	**22,500**	**18,500**	**-4,000**

Year 2

No.	Description	Planed	Used	Diff.
1	Wind Tunnel Models and Components	-	-	-
2	Force Measurement Equipment	-	-	-
3	Wind Tunnel Cost (Wind Generator)	2,000	(8,000)	+6,000
4	Engineering and Technician Support (Engineering Support)	1,500	(1,500)	-
5	Students / Research Assistants (Student 500*6)	5,000	(3,000)	-2,000
6	Researcher (Principal Researcher)	4,000	(4,000)	-
7	Report and Office Tools (Student and Office Material)	1,250	(1,250)	-
8	Transportations (Transportation in 2nd year)	1,500	(1,500)	-
9	Conference and Related Expense (For AIAA2024)	5,000	(5,000)	-
10	University Fees (University Free)	2,250	(2,250)	-
	Total	**22,500**	**26,500**	**+4,000**